

University of Dundee

Phytophthora infestans RXLR effectors target parallel steps in an immune signal transduction pathway

Ren, Yajuan; Armstrong, Miles; Qi, Yetong; McLellan, Hazel; Zhong, Cheng; Du, Bowen

Published in:
Plant Physiology

DOI:
[10.1104/pp.18.00625](https://doi.org/10.1104/pp.18.00625)

Publication date:
2019

Document Version
Peer reviewed version

[Link to publication in Discovery Research Portal](#)

Citation for published version (APA):

Ren, Y., Armstrong, M., Qi, Y., McLellan, H., Zhong, C., Du, B., ... Tian, Z. (2019). Phytophthora infestans RXLR effectors target parallel steps in an immune signal transduction pathway. *Plant Physiology*, 180(4), 2227-2239. <https://doi.org/10.1104/pp.18.00625>

General rights

Copyright and moral rights for the publications made accessible in Discovery Research Portal are retained by the authors and/or other copyright owners and it is a condition of accessing publications that users recognise and abide by the legal requirements associated with these rights.

- Users may download and print one copy of any publication from Discovery Research Portal for the purpose of private study or research.
- You may not further distribute the material or use it for any profit-making activity or commercial gain.
- You may freely distribute the URL identifying the publication in the public portal.

Take down policy

If you believe that this document breaches copyright please contact us providing details, and we will remove access to the work immediately and investigate your claim.

1 **Short title:** Different effectors disable the same signal pathway.

2 **Article Title:** *Phytophthora infestans* RXLR effectors target parallel steps in an
3 **immune signal transduction pathway**

4 Yajuan Ren^{1,2}, Miles Armstrong^{3,4}, Yetong Qi^{1,2}, Hazel McLellan³, Cheng Zhong¹, Bowen
5 Du^{1,2}, Paul RJ Birch^{3,4§}, Zhendong Tian^{1,2§}

6 ¹Key Laboratory of Potato Biology and Biotechnology, Ministry of Agriculture and Rural
7 Affairs, Huazhong Agricultural University (HZAU), Wuhan 430070, People's Republic of
8 China

9 ²Key Laboratory of Horticultural Plant Biology (HZAU), Ministry of Education, Huazhong
10 Agricultural University, Wuhan 430070, People's Republic of China

11 ³Division of Plant Sciences, School of Life Science, University of Dundee (at James Hutton
12 Institute), Errol Road, Invergowrie, Dundee DD2 5DA, UK

13 ⁴Cell and Molecular Sciences, James Hutton Institute, Errol Road, Invergowrie, Dundee DD2
14 5DA, UK

15 **§ Authors for correspondence:** P.Birch@dundee.ac.uk; tianzhd@mail.hzau.edu.cn

16 **One sentence summary:** Two *P. infestans* effectors, PexRD2 and Pi22926, target two
17 parallel MAP3K proteins in the same signal transduction pathway to promote *P. infestans*
18 colonization.

19 **Author contributions:** Z.T and P.R.J.B conceived the research and designed the
20 experiments. M.A and C.Z performed the original yeast-2-hybrid screen. Y.Q performed *N.*
21 *benthamiana* transformations. Y.Q performed VIGS and cell death assay. B.D performed
22 late blight resistance assay. R.Y performed most of the experiments. Y.R and Z.T performed
23 data analysis and made figures. Y.R, M.H, P.R.J.B and Z.T. wrote the paper with
24 contributions of all the authors. Z.T. and P.R.J.B secured funding.

25 **Abstract**

26 The potato (*Solanum tuberosum*) blight pathogen *Phytophthora infestans* delivers
27 RXLR effector proteins into host cells to subvert plant immune responses and
28 promote colonization. We show that transient expression and stable transgenic
29 expression of the RXLR effector Pi22926 in *Nicotiana benthamiana* promotes leaf
30 colonization by *P. infestans*. Pi22926 suppresses cell death triggered by
31 co-expression of the *Cladosporium fulvum* avirulence protein Avr4 and the tomato
32 (*Solanum lycopersicum*) resistance protein Cf4. Pi22926 interacts with a potato
33 Mitogen Activated Protein Kinase Kinase Kinase, StMAP3K β 2, in the nucleoplasm.
34 Virus-induced gene silencing (VIGS) of the orthologue *NbMAP3K β 2* in *N.*
35 *benthamiana* enhances *P. infestans* colonization and attenuates Cf4/Avr4-induced
36 cell death, indicating that this host protein is a positive regulator of immunity. Cell
37 death induced by Cf4/Avr4 is dependent on NbMAP3K ϵ and NbMAP3K β 2, indicating
38 that these MAP3Ks function in the same signalling pathway. VIGS of *NbMAP3K β 2*
39 does not compromise cell death triggered by overexpression of MAP3K ϵ . Similarly,
40 VIGS of *NbMAP3K ϵ* does not attenuate cell death triggered by MAP3K β 2,
41 demonstrating that these MAP3K proteins function in parallel. In agreement, Pi22926
42 or another RXLR effector PexRD2 only suppress cell death triggered by expression
43 of StMAP3K β 2 or StMAP3K ϵ , respectively. Our data reveal that two *P. infestans*
44 effectors, PexRD2 and Pi22926, promote *P. infestans* colonization by targeting
45 MAP3K proteins that act in parallel in the same signal transduction pathway.

46 **Key words:** effector-triggered immunity; hypersensitive response; effector-triggered
47 susceptibility; late blight; oomycete

48

49 **Introduction**

50 Plants have a two-layer surveillance system to respond to pathogens and mount
51 defenses against attack (Jones and Dangl, 2006; Dodds and Rathjen, 2010). The
52 first layer is initiated at the host cell surface by pattern recognition receptors (PRRs)
53 that detect microbe-associated molecular patterns (MAMPs), such as bacterial
54 flagellin, elongation factor EF-Tu, peptidoglycans and lipopolysaccharide (Couto and
55 Zipfel, 2016). This detection system results in pattern-triggered immunity (PTI),
56 accompanied by activation of mitogen activated protein kinase (MAPK) signalling
57 cascades, production of reactive oxygen species (ROS), callose deposition in the cell
58 wall and the induction of pathogenesis-related (PR) protein expression (Chisholm et
59 al., 2006; Jones and Dangl, 2006). In turn, successful plant pathogens deliver a
60 range of effector proteins that act in the apoplast or within plant cells to attenuate PTI.
61 Our understanding of how effectors manipulate host targets to interfere with defense
62 pathways and processes has been led by the studies of bacterial type III secreted
63 effectors (Dou and Zhou, 2012; Block and Alfano, 2011; Deslandes and Rivas, 2012).
64 More recently, the targets of effectors from filamentous plant pathogens such as
65 fungi and oomycetes have been revealed (Toruño et al., 2016; Whisson et al 2016;
66 Anderson et al., 2015). Plants possess resistance (R) proteins which perceive
67 effectors or effector activities, leading to effector-triggered immunity (ETI). This
68 causes rapid and localized programmed cell death (PCD), ROS production and
69 prolonged MAPK activation (Jones and Dangl, 2006).

70 The MAPK cascade is a core module for signal transduction in response to
71 extracellular stimuli in plants. MAPK pathways play important roles in activation of
72 plant immune responses mediated by both PRR and R proteins (Pedley and Martin,
73 2005; Pitzschke et al., 2009). MAPK pathways generally include three protein
74 kinases: MAP kinase kinase kinase (MAP3K), MAP kinase kinase (MAP2K) and
75 MAP kinase (MAPK). The MAPK is phosphorylated by a MAP2K, which itself is
76 phosphorylated by a MAP3K. In the *Arabidopsis thaliana* genome, there are at least
77 20 putative MAPKs, 10 MAP2Ks, and more than 80 MAP3Ks (Pitzschke et al., 2009).

78 MAP3Ks can be divided into a further 3 groups. These are the MEKK (MAPK/ERK
79 kinase kinase)-like subgroup which function as MAP3Ks in plants and mainly
80 participate in linear cascades and the ZIK-like and Raf-like groups, functional
81 characterization of which largely comes from organisms other than plants (MAPK
82 Group, 2002; Colcombet and Hirt, 2008). Only a limited number of MAP3Ks are
83 associated with regulating plant immunity. For example, Arabidopsis MEKK1 is
84 activated downstream of the PRR FLS2 which detects the bacterial MAMP flg22.
85 Studies have shown that MEKK1 regulates MEKK1-MKK1/2-MPK4, which negatively
86 regulates plant defense responses (Gao et al., 2008; Suarez-Rodriguez et al., 2007).
87 More recently, the MAP3Ks MAPKKK3 and MAPKKK5, which are activated by
88 receptor-like cytoplasmic kinase VII family members, are responsible for activating
89 the MAPKs MPK3/MPK6 (Bi et al., 2018). Conversely, the MAP3K YODA, which
90 promotes stomatal development, directly inhibits the MAPKKK3/MAPKKK5 activation
91 of MPK3/MPK6, demonstrating the antagonism that exists between plant growth and
92 immunity (Sun et al., 2018).

93 *Nicotiana benthamiana* MAP3K NPK1 is essential for regulating the resistance
94 responses mediated by the R proteins N, Bs2, and Rx, and may play roles in one or
95 more MAPK cascades (Jin et al., 2002). Tomato (*Solanum lycopersicum*) MAP3K α is
96 involved in two distinct MAPK cascades, either MEK2-SIPK or MEK1-NTF6, to
97 regulate plant immunity (del Pozo et al., 2004). Tomato MAP3K ϵ activates the
98 MEK2-SIPK/WIPK cascade to positively regulate defense (Melech-Bonfil and Sessa,
99 2010). Finally, the Arabidopsis Raf-like MAP3K EDR1 was found to negatively
100 regulate plant immunity (Frye et al., 2001).

101 Oomycete pathogens, ranging from obligate biotrophs to necrotrophs, deploy a
102 variety of apoplastic and intracellular effectors (Kamoun et al., 2015). The best
103 studied intracellular effectors are the RXLR class, which contain a signal peptide
104 followed by a conserved Arg-X-Leu-Arg (RXLR) motif. It has been reported that the
105 RXLR peptide motif acts as a host-targeting signal for translocation into host plant
106 cells to suppress plant immunity (Whisson et al., 2007; Dou et al., 2008). Recently,

107 delivery of RXLR effectors from the oomycete potato blight pathogen *Phytophthora*
108 *infestans* into plant cells has been visualized, revealing that they are secreted via a
109 non-canonical pathway (Wang et al., 2017; 2018a).

110 Since the bacterial type 3 effector HopA11 was shown to suppress activation of
111 MPK3 and MPK6 in Arabidopsis, a range of phytopathogen effectors have been
112 implicated in targeting MAPK pathways (Bi and Zhou, 2017). RXLR effectors from *P.*
113 *infestans* have been shown to suppress MAPK signaling cascades, or to interact with
114 MAP3K components to interfere with immunity (Whisson et al., 2016). Three RXLRs,
115 Pi13628/SFI5/PexRD27, Pi13959/SFI6 and Pi18215/SFI7/Avr3b are able to
116 suppress flg22-triggered MAMP signaling at, or upstream of, the MAPK cascade in
117 tomato (Zheng et al., 2014). The effector Pi11383/PexRD2 specifically targets the
118 kinase domain of MAP3K ϵ , directly inhibiting its activity to perturb plant defense
119 responses (King et al., 2014). Recently, Murphy et al. (2018) reported that the
120 effector Pi17316 interacts with the host MAP3K, StVIK, which acts as a susceptibility
121 (S) factor to enhance *P. infestans* colonization.

122 In this study we show that the *P. infestans* effector PITG_22926 (Pi22926) targets the
123 potato (*Solanum tuberosum*) MAP3K, StMAP3K β 2, a positive regulator of immunity,
124 to facilitate disease. Transient or stable expression of the RXLR effector Pi22926 in
125 the model host *N. benthamiana* promotes the growth of *P. infestans* and specifically
126 suppresses cell death induced by co-expression of the tomato resistance protein Cf4
127 with the *Cladosporium fulvum* avirulence protein Avr4. Pi22926 interacts with the
128 kinase domain of StMAP3K β 2 in a yeast two-hybrid (Y2H) library screen and *in*
129 *planta*. Virus-induced gene silencing (VIGS) of *MAP3K β 2* in *N. benthamiana*
130 enhanced *P. infestans* colonization and attenuated Cf4/Avr4-induced cell death,
131 indicating that it is a positive regulator of plant immunity. Overexpression of
132 StMAP3K β 2 or its kinase domain induced cell death in *N. benthamiana* which is
133 suppressed by Pi22926. Epistasis experiments revealed that StMAP3K β 2 acts in
134 parallel to StMAP3K ϵ , and upstream of MEK2. Our results reveal a *P. infestans*
135 effector protein that interacts with host StMAP3K β 2 to target the same signaling

136 pathway as PexRD2 for immune suppression.

137 **Results and Discussion**

138 **The RXLR effector Pi22926 promotes *P. infestans* colonization**

139 The RXLR effector gene *PITG_22926* (*Pi22926*) was shown previously to be
140 up-regulated at 2 and 3 days post *P. infestans* infection of potato leaves in both
141 genotype T30-4 and genotype 13_A2 (Haas et al., 2009; Cooke et al., 2012), and
142 more recently in diverse potato genotypes in China and during tuber infection (Yin et
143 al., 2017; Ah-Fong et al., 2017). Here, we confirmed that *Pi22926* is also
144 up-regulated in *P. infestans* isolate HB09-14-2 at 24, 48 and 72 h post-inoculation of
145 a Chinese potato variety 'E-potato-3' (Supplemental Figure S1). The time course
146 suggests that *Pi22926* contributes to the biotrophic phase of infection, similar to
147 other PiRXLR effectors (Whisson et al., 2016). Recently, *Pi22926* has been shown to
148 be secreted from *P. infestans* haustoria and delivered into host cells to accumulate in
149 the nucleus (Wang et al., 2018a), where it enhances *P. infestans* colonization of *N.*
150 *benthamiana* (Wang et al., 2018b). We confirmed that the disease lesion diameters
151 on the half leaves transiently expressing GFP-*Pi22926* (the signal peptide was
152 deleted) were significantly larger compared to the GFP control six days post-
153 inoculation (Supplemental Figure S2). The GFP-*Pi22926* fusion protein was intact
154 when transiently expressed in *N. benthamiana* leaves (Supplemental Figure S3A).

155 To explore this phenomenon further, transgenic *N. benthamiana* plants were made
156 for stable expression of GFP-*Pi22926*. *GFP-Pi22926* expression was detected in 4
157 transgenic lines (Supplemental Figure S4). All 4 lines showed growth and
158 morphology similar to wild type and 2 lines were thus taken forward for detailed study.
159 Leaves from transgenic plants were infected with *P. infestans* and were found to
160 sustain significantly larger *P. infestans* lesions compared to wild-type control plants
161 (Figure 1A, B). The GFP-*Pi22926* fusion protein was intact in transgenic *N.*
162 *benthamiana* leaves (Supplemental Figure S3C). These results reveal that
163 GFP-*Pi22926* activity within host cells is beneficial to *P. infestans* colonization.

164 **Pi22926 specifically suppresses Avr4/Cf4 and AvrPto/Pto triggered cell death**

165 Co-expression of the *C. fulvum* avirulence protein Avr4 and the tomato resistance
166 protein Cf4, or the *Pseudomonas syringae* avirulence protein AvrPto and
167 corresponding tomato resistance protein component Pto, triggers cell death in *N.*
168 *benthamiana* via activation of a common signaling pathway. The PiRXLR effector
169 PexRD2 was previously shown to specifically suppress Avr4/Cf4 and AvrPto/Pto
170 triggered cell death (King et al., 2014), and we confirmed these results as a positive
171 control in this study (Figure 2). In addition, our results reveal that Avr4/Cf4 and
172 AvrPto/Pto triggered cell death were significantly attenuated by co-expression with
173 Pi22926 compared with the empty vector control (Figure 2A, 2B). We also tested
174 whether Pi22926 is able to suppress cell death triggered by the *P. infestans* avirulence
175 protein (Avr3a^{KI}) and resistance protein R3a pairs (Armstrong et al., 2005), or potato
176 virus X (PVX) coat protein (PVX-CP) and PVX resistance protein (RX) pairs (Moffett
177 et al., 2002), and by *P. infestans* MAMP INF1 (Kamoun et al., 1998). No change to
178 the mean percentage of cell death mediated by these elicitors was observed in the
179 presence of Pi22926 (Figure 2B), indicating that they are independent of the signal
180 transduction cascade(s) manipulated by Pi22926 or PexRD2. These results indicate
181 that Pi22926 and PexRD2 may suppress the same specific signalling pathway to
182 promote disease.

183 **Pi22926 specifically targets potato MAP3K β 2**

184 To identify possible host targets of Pi22926, a yeast-2-hybrid (Y2H) library composed
185 of cDNA from potato plants infected with *P. infestans* (Bos et al., 2010) was screened
186 with Pi22926 as a bait. The screen involved approximately 1.2×10^6 yeast
187 co-transformants. Two yeast co-transformants growing on selection plates contained
188 identical, partial sequences corresponding to a potato MAP3K (XP_006349414.1).
189 Alignment of full-length amino acid sequences of MAP3Ks from potato, *N.*
190 *benthamiana* and tomato showed that the potato interacting protein shares high
191 identities with both a tomato protein (XP_004230523.1, identity: 94.59%) and a *N.*

192 *benthamiana* protein (Nbv6.1trP19888, identity: 82.64%). The tomato and potato
193 proteins were reciprocal best Blast hits (RBBHs), and thus candidate orthologues, of
194 NbMAP3K β 2 (Supplemental Figure S5). The potato interacting protein was hence
195 named StMAP3K β 2. StMAP3K β 2 contains a kinase domain at the C terminus
196 (residues 402 to 653) (Supplemental Figure S5).

197 To investigate the specificity of the interaction between Pi22926 and StMAP3K β 2, a
198 pairwise Y2H assay was performed in which the full length StMAP3K β 2, its active
199 kinase domain (KD), and an inactive form in which the active site lysine in the ATP
200 binding site (Lys 430) was substituted with an arginine, were used as prey clones
201 against the bait Pi22926. In addition, two other RXLR effectors, PexRD2 (Pi11383)
202 and Pi04089, were used as controls. PexRD2 targets another MAP3K in the
203 cytoplasm, StMAP3K ϵ (King et al., 2014) and Pi04089 shows a similar nuclear
204 localization to Pi22926 but interacts with the RNA binding protein StKRBP1 (Wang et
205 al., 2015). While all yeast transformants grew on control +His plates, the interactions
206 of Pi22926 with full length StMAP3K β 2 or with its active KD were indicated by
207 induction of β -galactosidase activity and growth on media lacking histidine (-His).
208 The Pi04089 or PexRD2 combinations did not activate either reporter (Figure 3A,
209 Supplemental Figure S6). In addition, whereas PexRD2 interacted with StMAP3K ϵ ,
210 no such interaction was observed between Pi22926 and StMAP3K ϵ (Supplemental
211 Figure S6). Importantly, the mutant StMAP3K β 2(KD)^{Lys430Arg} also failed to interact
212 with Pi22926 (Figure 3A). This suggests that the intact active kinase domain of
213 StMAP3K β 2 is necessary and sufficient for the specific interaction with Pi22926.

214 To confirm that specific interactions also occur *in vivo*, a co-immunoprecipitation
215 (co-IP) assay was performed by transiently co-expressing cMyc-StMAP3K β 2(KD) or
216 cMyc-StMAP3K β 2(KD)^{Lys430Arg} with GFP-Pi22926, or with the GFP-Pi04089 control,
217 following immunoprecipitation with GFP-TRAP_M beads. Intact GFP- or
218 cMyc-labelled proteins were all stably expressed when corresponding constructs
219 were transiently expressed in *N. benthamiana* leaves as indicated in the input
220 samples. The cMyc-StMAP3K β 2 (KD) was only pulled down in the presence of

221 Pi22926, but not with the Pi04089 control (Figure 3B). These results indicate that
222 Pi22926 specifically interacts with StMAP3K β 2 by its active kinase domain (KD) both
223 in yeast and *in planta*.

224 **Pi22926 interacts with StMAP3K β 2 in the nucleoplasm**

225 To investigate the subcellular localization of Pi22926 and StMAP3K β 2, GFP was
226 fused to their N or C terminus to form GFP-Pi22926 and StMAP3K β 2-GFP and
227 viewed following Agrobacterium-mediated expression in *N. benthamiana* using
228 confocal microscopy. GFP-Pi22926 localized predominantly in the nucleus and
229 nucleolus (Figure 4A). StMAP3K β 2-GFP localized in the cytoplasm and showed
230 weak fluorescence in the nucleoplasm, but was not observed in the nucleolus (Figure
231 4B). GFP-Pi22926 and StMAP3K β 2-GFP were stable as fusion proteins *in planta*
232 (Supplemental Figure S3A, B). When RFP-Pi22926 and StMAP3K β 2-GFP were
233 co-expressed by Agrobacterium-mediated expression in *N. benthamiana*,
234 RFP-Pi22926 and StMAP3K β 2-GFP were co-localized in the nucleus (Figure 4C),
235 but StMAP3K β 2-GFP still retained cytoplasmic fluorescence background. We thus
236 investigated the interaction using bimolecular fluorescence complementation. When
237 YN-Pi22926 and YC-StMAP3K β 2 were co-expressed by Agrobacterium-mediated
238 expression in *N. benthamiana*, reconstituted YFP fluorescence was observed only in
239 the nucleoplasm (Figure 4D). By contrast, when YC-StMAP3K β 2 was co-expressed
240 with YN-Pi04089 (Wang et al., 2015), only weak background fluorescence was
241 observed (Figure 4E). YN-Pi22926, YN-Pi04089 and YC-StMAP3K β 2 were stable as
242 fusion proteins *in planta* (Supplemental Figure S3D, E). This demonstrates that the
243 interaction between these proteins occurs in the nucleoplasm, despite both showing
244 some level of cytoplasmic localization. Further work is needed to look at substrates
245 of StMAP3K β 2 and where it phosphorylates them. Interestingly, StMAP3K ϵ and
246 PexRD2 interacted in the cytoplasm, suggesting that there are alternative substrates
247 for phosphorylation at that location that contribute to cell death (King et al., 2014).

248 **Silencing of *NbMAP3K β 2* promotes *P. infestans* colonization**

249 To investigate the potential role of StMAP3K β 2 in plant defense responses to *P.*
250 *infestans*, VIGS was employed to knock-down the expression of *NbMAP3K β 2*
251 (orthologue of *StMAP3K β 2*) in the model host plant *N. benthamiana*. We confirmed
252 that GFP-Pi22926 is able to interact with the kinase domains of both StMAP3K β 2
253 and NbMAP3K β 2 in yeast and *in planta* (Supplemental Figure S7A, B). Two VIGS
254 vectors containing independent portions of the *NbMAP3K β 2* gene,
255 TRV:NbMAP3K β 2-5' and TRV:NbMAP3K β 2-3', were generated to specifically knock
256 down this gene in *N. benthamiana* (Supplemental Figure S8A). Transcript levels of
257 the target gene in plants expressing each of the TRV:NbMAP3K β 2 constructs was
258 reduced by 70%-80%, but *NbMAP3K ϵ* transcript levels were unaltered
259 (Supplemental Figure S8B). VIGS plants showed a developmentally normal
260 phenotype when compared with the TRV:GFP control. TRV:NbMAP3K β 2 and
261 TRV-GFP plants were infected with *P. infestans* isolate 88069. Seven days
262 post-inoculation (dpi), measurements of both *P. infestans* lesion diameter and
263 sporangia production on TRV:GFP and TRV:NbMAP3K β 2-5' and
264 TRV:NbMAP3K β 2-3'-expressing *N. benthamiana* plants showed that silencing of
265 *NbMAP3K β 2* significantly enhanced *P. infestans* colonization compared with the
266 TRV:GFP control (Figure 5A, B, C). This indicates that NbMAP3K β 2 is potentially a
267 positive regulator of plant immunity.

268 **Cell death induced by Avr4/Cf4 and AvrPto/Pto is dependent on MAP3K β 2**

269 As Pi22926 suppresses Cf4/Avr4 and Pto/AvrPto cell death, we hypothesised that
270 MAP3K β 2 may act in the signal transduction pathways leading to these cell death
271 responses. To test that, TRV:NbMAP3K β 2-5' and TRV:NbMAP3K β 2-3' were used to
272 silence *NbMAP3K β 2* in *N. benthamiana* plants, and the leaves of VIGS plants were
273 infiltrated with the *Agrobacterium tumefaciens* harboring effector/R protein pairs
274 Avr4/Cf4 and AvrPto/Pto. As expected, similar to the silencing of *MAP3K ϵ* (specific
275 silencing efficiency shown in Supplemental Figure S9), we observed that silencing of
276 *NbMAP3K β 2* significantly reduced the percentage of sites developing cell death

277 upon co-expression of Avr4/Cf4 or AvrPto/Pto, compared with the TRV:GFP empty
278 vector control (Figure 6). However, silencing of *NbMAP3Kβ2* and *NbMAP3Kε* did not
279 compromise INF1, Avr3a/R3a or RX/CP triggered cell death (Supplemental Figure
280 S10), indicating that silencing of *NbMAP3Kβ2* specifically compromises Avr4/Cf4 or
281 AvrPto/Pto triggered cell death. Taken together, our results suggest that
282 *NbMAP3Kβ2*, like *MAP3Kε* (King et al., 2014), plays an essential role in the signaling
283 pathway activated by Avr4/Cf4 or AvrPto/Pto.

284 **Pi22926 suppresses cell death induced by expression of StMAP3Kβ2 and its** 285 **kinase domain**

286 Expression of the full length and kinase domain (KD) of some MAP3Ks in *N.*
287 *benthamiana* induces cell death (Hashimoto et al., 2012). To determine whether
288 overexpression of StMAP3Kβ2 is able to induce cell death, we used *Agrobacterium*
289 to transiently express the full length StMAP3Kβ2, its active KD, or the inactive form
290 (KD)^{Lys430Arg} in *N. benthamiana* leaves. We observed that overexpression of
291 StMAP3Kβ2 or its KD alone resulted in pathogen- and elicitor-independent cell death
292 compared to the GFP control. In contrast, cell death was not observed in leaves
293 expressing inactive KD^{Lys430Arg}, suggesting that an intact kinase catalytic domain is
294 essential for StMAP3Kβ2 to trigger cell death (Figure 7A, C). As Pi22926 was shown
295 to interact with StMAP3Kβ2 (Figure 3), this prompted us to test whether Pi22926 has
296 any effect on the cell death induced by StMAP3Kβ2. We co-expressed GFP-Pi22926
297 with StMAP3Kβ2 or its KD in *N. benthamiana* using *Agrobacterium*-mediated
298 expression. Seven days post-agroinfiltration, we observed that StMAP3Kβ2- and
299 KD-induced cell death was significantly suppressed by co-expression with
300 GFP-Pi22926 compared to the GFP control. This indicates that Pi22926 is a
301 suppressor of cell death triggered by StMAP3Kβ2 (Figure 7B, D).

302 **MEK2 and SIPK act downstream of StMAP3Kε and StMAP3Kβ2**

303 To test whether StMAP3Kε and StMAP3Kβ2 share the same downstream signaling

304 cascade, VIGS constructs that silence *MEK1* and *MEK2* (encoding MAP2Ks), or
305 constructs for silencing wound-induced protein kinase gene *WIPK*, salicylic
306 acid-induced protein kinase gene *SIPK* or *NTF6* (MAPKs) were generated and used
307 to silence corresponding genes in *N. benthamiana* plants. The efficiency of silencing
308 was assessed by RT-qPCR analysis that measured the expression of each target
309 gene in silenced plants relative to control TRV:GFP plants (Supplemental Figure
310 S11). Typical cell death was observed on the leaves of TRV:GFP control plants when
311 expressing intact KDs of StMAP3K ϵ and StMAP3K β 2, but mutated KDs (as a
312 negative control) did not induce cell death (Figure 8A). Intact KDs of StMAP3K ϵ and
313 StMAP3K β 2 were also able to induce cell death in both TRV: *MEK1* and TRV:*NTF6*
314 VIGS plants (Figure 8A). However, silencing of *MEK2*, *WIPK* and *SIPK* significantly
315 inhibited the cell death triggered by the expression of intact KDs of StMAP3K ϵ
316 (Figure 8A, B). This result is in agreement with the tomato SIMAP3K ϵ which
317 mediated a cell death signaling cascade involving the MAP2K MEK2 and the two
318 MAPKs WIPK and SIPK rather than MEK1 or NTF6 (Melech-Bonfil and Sessa, 2010).
319 Interestingly, although the cell death triggered by StMAP3K β 2 needed MEK2 and
320 SIPK, similar to StMAP3K ϵ , silencing WIPK did not abolish StMAP3K β 2 triggered
321 cell death (Figure 8A, C). This indicates that StMAP3K ϵ and StMAP3K β 2 share the
322 same signal transduction pathway but there is a difference downstream of MEK2.

323 **Pi22926 suppresses StMAP3K β 2-triggered cell death but does not suppress**
324 **StMAP3K ϵ -triggered cell death**

325 A previous study reported that the *P. infestans* RXLR effector PexRD2 suppresses
326 cell death triggered by activity of the kinase domain of MAP3K ϵ (King et al., 2014).
327 We show that Pi22926 suppresses StMAP3K β 2(KD) triggered cell death, whereas
328 the effectors PexRD2, Pi13959, Pi13628 and Pi18215 failed to do so (Figure 9A, B).
329 To test whether Pi22926 suppresses StMAP3K ϵ -triggered cell death, Pi22926 and
330 StMAP3K ϵ (KD) were transiently co-expressed in *N. benthamiana*. We found that
331 Pi22926 cannot suppress StMAP3K ϵ (KD)-triggered cell death, whereas PexRD2

332 does (Figure 9C, D). These results indicate that StMAP3K β 2 and StMAP3K ϵ likely
333 act at the same level in the cell death signalling pathway.

334 **StMAP3K β 2 acts in parallel with StMAP3K ϵ in Cf4/AVR4 induction of cell death**

335 Epistasis analysis of the functional relationships among NbMAP3K β , NbMAP3K γ ,
336 and NbMAP3K α suggested that these three MAP3Ks form a linear signalling
337 pathway which proceeds from NbMAP3K β to NbMAP3K γ to NbMAP3K α to lead to
338 cell death (Hashimoto et al., 2012). We have shown that NbMAP3K β 2 and MAP3K ϵ
339 are involved in the same signalling pathway in that they positively regulate Avr4/Cf4
340 and AvrPto/Pto signal transduction (Figure 6). The observation that Pi22926 or
341 PexRD2 can only suppress cell death during transient co-expression with
342 NbMAP3K β 2 or MAP3K ϵ , respectively, suggests that MAP3K ϵ and NbMAP3K β 2
343 may function at the same level in the signal transduction pathway.

344 To confirm this, we silenced each gene using VIGS in *N. benthamiana*. Silencing of
345 *NbMAP3K β 2* did not significantly (ANOVA, $p < 0.001$) suppress MAP3K ϵ triggered cell
346 death (Figure 9E) compared to the TRV:GFP control. VIGS of *NbMAP3K ϵ* did not
347 suppress the cell death induced by transient expression of NbMAP3K β 2 (Figure 9F).
348 Taken together, these results confirm that MAP3K ϵ and MAP3K β 2 act in parallel in
349 the same signalling pathway in Cf4/AVR4 cell death induction.

350 Perception of the *P. infestans* MAMP INF1 triggers a MAPK pathway that is
351 independent of MAP3K ϵ and MAP3K β 2, and is thus not suppressed by the effectors
352 PexRD2 (King et al., 2014) or Pi22926. In contrast, as yet unidentified receptor(s)
353 activated by unknown *P. infestans* elicitor(s) trigger a MAPK cascade that includes
354 StMAP3K ϵ and StMAP3K β 2, resulting in activation of MAP2K MEK2 and finally
355 SIPK/WIPK (Figure 10), ultimately leading to cell death. The importance of the
356 StMAP3K ϵ /StMAP3K β 2-MEK2-SIPK/WIPK pathway in immunity to *P. infestans* is
357 highlighted by the fact that these two RXLR effectors from distinct MCL cluster
358 families (Haas et al., 2009), PexRD2 (RXLRfam6) and Pi22926 (RXLRfam52), which

359 act to suppress parallel regulatory steps (Figure 10).

360 Future work will reveal whether other *P. infestans* RXLRs target additional members
361 of this MAPK cascade to redundantly suppress this immune pathway, or indeed may
362 target additional MAPK signal transduction pathways associated with immune
363 responses. In the large-scale effector yeast-2-hybrid screens of Mukhtar et al. (2011)
364 and Weßling et al. (2014) MAPK signaling components did not emerge as ‘hubs’ that
365 are targeted by effectors from different pathogens. Nevertheless, type III effectors
366 from bacterial plant pathogens, such as hopA11 from *P. syringae*, which targets
367 MPK3 and MPK6, can also directly inactivate MAPK cascade components that
368 positively regulate immunity. Moreover, the *P. syringae* effector AvrB targets MPK4 to
369 promote its activity as a negative regulator of immunity (Cui et al., 2010), and the *P.*
370 *infestans* effector Pi17316 targets the susceptibility factor VIK, also to exploit its role
371 as a negative immune regulator (Murphy et al., 2018). Thus bacterial and oomycete
372 effectors directly target both positive and negative regulators of immunity within
373 MAPK cascades.

374 In conclusion, this study emphasizes the power of effectors as probes to dissect and
375 understand the regulation of plant immune signaling pathways. However, the PRR
376 that perceives a *P. infestans* molecule to initiate the
377 StMAP3K ϵ /StMAP3K β 2-MEK2-SIPK/WIPK pathway is unknown, highlighting the
378 need to more deeply invest in identifying cell surface receptors and the pathogen
379 ligands that they detect to activate defence.

380 **Materials and methods**

381 **Plant materials**

382 *Nicotiana benthamiana* plants were grown in individual plots in the greenhouse with
383 16 h days at 22 °C and 8 h nights at 18 °C. Approximately 4–5-week-old *N.*
384 *benthamiana* were used for experiments. A Chinese potato (*Solanum tuberosum*)

385 variety 'E-potato-3' was used for *Pi22926* expression tests. *In vitro* cultured plantlets
386 were grown in the greenhouse as above. Leaves from 8 weeks old plants were used
387 for *Phytophthora infestans* inoculation.

388 **Plasmid construction**

389 The RXLR effectors *Pi22926* and *Pi04089* were cloned without signal peptides from
390 genomic DNA of *P. infestans* isolate T30-4 in a two-step PCR to add flanking attB
391 sites to the coding sequences. The potato StMAP3K β 2 coding sequence was
392 amplified from the original yeast-2-hybrid (Y2H) prey library using the same strategy.
393 The Y2H library was the same as that used by McLellan et al. (2013) and Yang et al.
394 (2016).

395 The PCR products were purified and cloned into pDONR221 (Invitrogen) to generate
396 entry clones via BP reactions. The effector entry clones were transferred into
397 pB7WGF2 (for N-terminal eGFP fusion), pK7WGR2 (for N-terminal RFP fusion), and
398 pDEST32 (for Y2H, Invitrogen). The StMAP3K β 2 and StMAP3K β 2 (KD) were
399 recombined with pK7FWG2 (for C-terminal eGFP fusion) and pDEST22 (for Y2H;
400 Invitrogen). For N-terminal cMyc tagging, pH7LIC was generated using the
401 ClonExpress Entry One Step Cloning Kit (Vazyme, Vazyme Biotech Co, Ltd, China).
402 For splitYFP constructs, *Pi04089* and *Pi22926* were recombined with pCL112 (for
403 N-terminal YN- fusion). StMAP3K β 2 was recombined with pCL113 (for N-terminal
404 YC- fusion).

405 Site-directed mutation of Lys430Arg in the StMAP3K β 2 kinase catalytic domain was
406 introduced using the Mut Express II Fast Mutagenesis Kit (Vazyme). The entry clone
407 containing the mutated form of StMAP3K β 2 was recombined into pDEST22 for Y2H
408 and pK7FWG2 for *in planta* assays. For N-terminal tagging with the cMyc epitope,
409 pH7LIC was generated for Co-immunoprecipitation analyses. Primer sequences
410 used for PCR amplification and vector construction are shown in Supplemental Table
411 S1.

412 ***N. benthamiana* transformation**

413 *Agrobacterium tumefaciens* containing overexpression vector pB7WGF2 was used
414 to transform leaf discs of *N. benthamiana*. Positive lines were first screened on
415 differential medium (MS + 2 mg/L 6-BA + 0.2 mg/L NAA + 1.5 mg/L Bialaphos (sodium
416 salt) + 400 mg/L Cef + 30 g/L sucrose, pH 5.7) and then transferred to root
417 generation medium (MS + 0.36 mg/L Bialaphos (sodium salt) + 200 mg/L Cef + 0.1
418 mg/L NAA + 30 g/L sucrose, pH 5.7). The positive lines were confirmed by
419 semi-quantitative RT-PCR. Primers are shown in Supplemental Table S1).

420 **Agro-infiltration and *P. infestans* infection assay**

421 *A. tumefaciens* strain GV3101 harboring plasmid constructs were grown overnight in
422 YEB medium with appropriate antibiotics at 28 °C at 200 rpm. The bacteria was
423 pelleted, resuspended in sterile 10 mM MES; 10 mM MgCl₂ and 200 μM
424 acetosyringone, and subsequently adjusted to the appropriate final OD₆₀₀ before
425 pressure infiltration into *N. benthamiana* leaves (generally 0.1 for infection assays,
426 0.3–0.5 for cell death and 0.5–1.0 for western blot and co-immunoprecipitation
427 assays). For co-expression, agrobacteria cultures containing the appropriate vector
428 constructs were mixed at a 1:1 ratio before infiltration. Each assay consisted of at
429 least 8 plants inoculated on 3–4 leaves.

430 *P. infestans* strain 88069 was grown on Rye Sucrose Agar (RSA) plates at 18 °C in
431 the dark for 14 days. Sporangia were harvested from RSA plates by adding 3 mL
432 H₂O to the plates and zoospores were collected after one hour of incubation at 4 °C.
433 Droplets (10 μL) of a solution of 100, 000 zoospores per mL were applied onto the
434 abaxial side of detached *N. benthamiana* leaves and incubated for several days on
435 wet paper towels in 100% relative humidity. *Agrobacterium tumefaciens* Transient
436 Assays (ATTA) in combination with *P. infestans* infection were carried out as
437 described (McLellan et al., 2013). For VIGS, the mean lesion diameter was
438 measured at 7 dpi and compared to the GFP control. Sporangia counts were
439 performed on 10 dpi leaves from VIGSed plants which had been washed in 5 ml H₂O
440 and vortexed to release sporangia. The number of sporangia recovered from each
441 leaf was counted using a hemocytometer.

442 **Yeast-two-hybrid**

443 A Y2H screen with pDEST32-Pi22926 was performed as described (McLellan et al.,
444 2013) using the ProQuest two-hybrid system (Invitrogen). The coding sequence of
445 StMAP3K β 2, StMAP3K β 2(KD) and StMAP3K β 2(KD)^{Lys430Arg} were recombined into
446 pDEST22 and re-tested with pDEST32-Pi22926 (pDEST32-Pi04089 as negative
447 control) in pairwise interactions. The transformants were selected using
448 SD/-Leu-Trp-His selective medium and X-gal assay to detect the reporter gene
449 activation.

450 **Co-immunoprecipitation**

451 Leaves of 5-week-old *N. benthamiana* were respectively agro-infiltrated with
452 GFP-Pi22926 (GFP-Pi040489 as a negative control), cMyc-tagged StMAP3K β 2(KD)
453 and cMyc-tagged StMAP3K β 2(KD)^{Lys430Arg}. Two days after agro-infiltration, four leaf
454 discs (9 mm in diameter) were harvested and proteins were extracted. GFP tagged
455 Pi22926/ Pi04089 fusions were immunoprecipitated using GFP-Trap-M magnetic
456 beads (MBL Biological Laboratories Co., Ltd. URL). The resulting samples were
457 separated by SDS-PAGE and western blotted. Immunoprecipitated GFP fusions and
458 co-immunoprecipitated c-Myc fusions were detected using appropriate antisera
459 (Sungene Biotech, China).

460 **Confocal microscopy**

461 *A. tumefaciens* ($OD_{600}=0.03-0.1$) containing target protein fusions were infiltrated into
462 leaves of 4-week old *N. benthamiana* plants. *N. benthamiana* leaf cells expressing
463 fluorescent protein fusions were imaged no later than 2 days after agroinfiltration
464 using a CLSM (Leica TCS-SPE, Germany) confocal microscope. GFP was excited
465 with 488 nm from an argon laser and its emissions were detected between 500 and
466 530 nm. mRFP was excited with 561 nm and its emissions were detected between
467 600 and 630 nm. Split-YFP was excited using 514 nm from an argon laser with
468 emissions detected from 530 to 575 nm. Images were collected from leaf cells
469 expressing low levels of the fluorescence to minimize artefacts of ectopic protein

470 expression.

471 **Virus Induced Gene Silencing**

472 Plasmids pTRV1 and pTRV2 were used for VIGS (Liu et al., 2002; Ekengren et al.,
473 2003). Constructs pTRV2:NbSIPK, pTRV2:NbWIPK, pTRV2:NbMEK1, pTRV2:
474 NbMEK2 and pTRV2: NbNTF6 were generated using the same gene fragments
475 based on the construct information previously published (Asai et al., 2008 ;
476 Melech-Bonfil and Sessa, 2010). pTRV2: NbMAPKKK ϵ -5' and pTRV2:
477 NbMAPKKK ϵ -3' used in this study have been described (Melech-Bonfil and Sessa,
478 2010). For pTRV2: NbMAP3k β 2, 300 bp PCR fragments were cloned from *N.*
479 *benthamiana* cDNA and inserted to pBinary Tobacco Rattle Virus (TRV) vectors (Liu
480 et al., 2002) between *Bam*H I and *Eco*R I sites in the antisense orientation. A TRV
481 construct expressing GFP described previously was used as a control (McLellan et
482 al., 2013). *A. tumefaciens* strains harboring pTRV2 vectors combined with that
483 harboring the pTRV1 vector were mixed at a 1:1 ratio and adjusted to OD₆₀₀=0.5.
484 The co-cultures were then infiltrated into two primary leaves of a plant at the
485 4-leaf-stage. Plants were used for assays or to check gene silencing levels by
486 RT-qPCR 2-3 weeks later. The primers and constructs used in this study are shown
487 in Supplemental Table S1.

488 **Gene expression assay**

489 Three leaf discs (9 mm in diameter) were collected from *N. benthamiana* VIGS plants
490 to extract total RNA using the PLANTpure Plant RNA Kit (Aidlab Biotechnologies,
491 China). The first strand cDNA was synthesized from 2 μ g of RNA using the
492 TRUEScript 1st Strand cDNA Synthesis Kit With gDNA Eraser (Aidlab
493 Biotechnologies, China). RT-qPCR reactions were performed using Power SYBR
494 Green (Bio-Rad, USA). The *N. benthamiana* gene *EF1 α* was used as a reference
495 control. Primer pairs were designed outside the region of the cDNA targeted for
496 silencing. The primers are shown in Supplemental Table S1. Gene expression levels
497 were calculated by a comparative $\Delta\Delta$ Ct method as described by Bio-Rad instruction.

498 **Statistical analyses**

499 All data and statistical analysis were carried out using one-way ANOVA and pairwise
500 or multiple comparisons in Graphpad Prism 6.0 software (GraphPad Prism Software
501 Inc., San Diego, CA, USA). All values and error bars presented are means and
502 standard deviation (SD) or standard error (SE) of three or more experimental
503 replicates.

504

505 **Accession Numbers**

506 Sequence data from this article can be found in the GenBank and website under the
507 following accession numbers. *P. infestans* PITG_22926 (EEY57148), PexRD2
508 (EEY62542); potato StMAP3K β 2 (XP_006360216.1), StMAP3K ϵ (KJ504180);
509 Tomato SIMAPKKK β 1 (XP_010323778.1), SIMAPKKK β 2 (XP_004230523.1). *N.*
510 *benthamiana* NbMAPKKK β (BAM36967.1), NbMAP3K β 2 (Nbv6.1trP19888,
511 <http://benthgenome.qut.edu.au/>), NbMAP3K ϵ (ADK36643 and BAM36969).

512

513 **Supplemental Materials**

514 **Supplemental Figure S1.** Expression of *Pi22926* in a *P. infestans* infection time
515 course on potato plants.

516 **Supplemental Figure S2.** The RXLR effector *Pi22926* enhances *P. infestans*
517 colonization of *N. benthamiana* leaves following Agrobacterium-mediated expression
518 compared to a GFP control.

519 **Supplemental Figure S3.** Stability of the target proteins labeled by different tags in
520 *N. benthamiana*.

521 **Supplemental Figure S4.** Expression of *Pi22926* in stable transgenic *N.*

522 *benthamiana* lines tested by RT-PCR.

523 **Supplemental Figure S5.** Alignment of MAP3K β 2s from tomato, potato and *N.*
524 *benthamiana*.

525 **Supplemental Figure S6.** Pi22926 does not interact with StMAP3K ϵ (KD) in yeast.

526 **Supplemental Figure S7.** Pi22926 interacts with NbMAP3K β 2(KD) in yeast and *in*
527 *planta*.

528 **Supplemental Figure S8.** NbMAP3K β 2 constructs and silencing efficiency.

529 **Supplemental Figure S9.** Silencing efficiency of *NbMAP3K ϵ* .

530 **Supplemental Figure S10.** Cell death responses in *MAP3K β 2* silenced *N.*
531 *benthamiana* plants.

532 **Supplemental Figure S11.** *MEK1*, *MEK2*, *SIPK*, *WIPK* and *NTF6* silencing
533 efficiency in *N. benthamiana* plants.

534 **Supplemental Table S1.** Primers and constructs used in this study.

535

536 **Acknowledgements**

537 We are grateful for financial support from the National Natural Science Foundation of
538 China (Grants No. 31761143007, 31471550) and the Fundamental Research Funds
539 for the Central Universities of China (Grant No. 2662017PY069), for funding ZT's lab,
540 the Biotechnology and Biological Sciences Research Council (BBSRC) (grants
541 BB/G015244/1, BB/K018183/1, BB/L026880/1) for PRJB, HM, MA, and The Scottish
542 Government Rural and Environment Science and Analytical Services Division
543 (RESAS) for funding PRJB.

544 **Figure Legends**

545 **Figure 1. The RXLR effector Pi22926 enhances *P. infestans* colonization of *N.***
546 ***benthamiana* leaves.** (A) Representative images taken under UV light at 5 days
547 after inoculation show that transgenic lines overexpressing GFP-Pi22926 enhance
548 pathogen colonization compared to the untransformed *N. benthamiana* control.
549 Scale bar represents 1 cm. (B) Graph shows a significant increase in *P. infestans*
550 lesions in transgenic lines overexpressing GFP-Pi22926 compared to wild type *N.*
551 *benthamiana* control (ANOVA, $p < 0.001$, 3 reps, $n = 120$). Lowercase letters on graphs
552 denote statistically significant groups. Error bars represent \pm SE.

553 **Figure 2. Pi22926 specifically suppresses Avr4/Cf4 and AvrPto/Pto induced cell**
554 **death.** (A) Representative leaf image taken under UV light at 5 days showing
555 Avr4/Cf4 and AvrPto/Pto cell death with EV, Pi22926 and PexRD2 positive control. (B)
556 Graph showing Pi22926 and PexRD2 expression lead to a significant decrease
557 ($p < 0.001$, 3 reps, $n = 94$) in cell death percentage triggered by Avr4/Cf4 and AvrPto/Pto.
558 Lowercase letters on graphs denote statistically significant groups by one-way
559 ANOVA, with pairwise comparisons performed with the Holm-Sidak method. Error
560 bars represent \pm SE.

561 **Figure 3. Pi22926 interacts with the kinase domain of StMAP3K β 2 in Y2H and**
562 **immunoprecipitation assays.** (A) Yeast co-expressing Pi22926 with StMAP3K β 2
563 and its kinase domain grow on –histidine (-HIS) medium and had β -galactosidase
564 (β -gal) activity, whereas those co-expressed with the inactive mutant kinase domain
565 StMAP3K β 2(KD)^{Lys430Arg} or the control Pi04089 did not. (B) Co-immunoprecipitation
566 from leaf extracts using GFP-trap (GFP IP) confirmed that cMyc tagged StMAP3K β 2
567 KD specifically interacted with GFP-Pi22926 and not with Pi04089. Expression of
568 constructs is indicated by +. Protein size markers are indicated in kDa, and protein
569 loading is indicated by Coomassie brilliant blue (CBB) staining.

570

571 **Figure 4. Pi22926 interacts with StMAP3K β 2 in nucleoplasm.** (A) Confocal
572 images show that GFP-Pi22926 is localized in the nucleoplasm and nucleolus. (B)

573 StMAP3K β 2-GFP is localized in the cytoplasm and nucleoplasm. For images of
574 StMAP3K β 2-GFP, the left one is a Z-stack, whereas the right one with higher
575 magnification is a single optical section from the stack. (C) Images show transient
576 co-expression of StMAP3K β 2-GFP with RFP-Pi22926. (D) Images show transient
577 co-expression of YC-StMAP3K β 2 with YN-Pi22926. Inset image is a nucleus at
578 higher magnification. (E) Images show transient co-expression of YC-StMAP3K β 2
579 with YN-Pi04089. Scale bars represent 10 μ m. OD₆₀₀ of Agrobacteria suspension for
580 GFP and RFP constructs is 0.1 and 0.03 for split YFP.

581

582 **Figure 5. Silencing of *NbMAP3K β 2* enhances *P. infestans* leaf colonization.** (A)
583 Images taken at 7 days after sporangia inoculation indicate more pathogen
584 colonization on TRV:*NbMAP3K β 2* plants compared to the TRV:GFP control. Scale
585 bar represents 1 cm. (B) Graph shows a significant increase (ANOVA, $p < 0.001$, 3
586 reps, $n = 120$) in *P. infestans* lesion diameter in plants expressing TRV:*NbMAP3K β 2-3'*
587 and TRV:*NbMAP3K β 2-5'*, compared with a TRV-GFP control. (C) Graph shows an
588 increase in the average numbers of sporangia mL^{-1} collected from infected leaves
589 expressing TRV:*NbMAP3K β 2-3'* and TRV:*NbMAP3K β 2-5'*, compared with a
590 TRV:GFP control (ANOVA, $p < 0.001$, 3 reps, $n = 120$). Lowercase letters on graphs
591 denote statistically significant groups. Error bars represent \pm SE.

592

593 **Figure 6. Cell death induced by *Avr4/Cf4* and *Avrpto/Pto* is dependent on**
594 **MAP3K ϵ and *NbMAP3K β 2*.** (A) Graph showing a significant suppression of cell
595 death (ANOVA, $p < 0.001$, 3 reps, $n = 72$) induced by *Avr4/Cf4* in *NbMAP3K β 2* silenced
596 plants, and in positive control *NbMAP3K ϵ* silenced plants, compared to TRV2:GFP
597 control. (B) Graph showing a significant decrease of cell death (ANOVA, $p < 0.001$, 3
598 reps, $n = 72$) triggered by *Avrpto/Pto* in *NbMAP3K β 2* silenced plants, and positive
599 control *NbMAP3K ϵ* silenced plants, compared to TRV2:GFP control. Error bars
600 represent \pm SE. Cell death numbers were counted at 6 days. Stars indicate
601 significant difference to the TRV:GFP control.

602

603 **Figure 7. Overexpression of StMAP3K β 2 or its kinase domain induces cell**
604 **death that is suppressed by Pi22926.** (A) Images taken under UV light at 7 days
605 after inoculation showing that transient overexpression of StMAP3K β 2 and its kinase
606 domain induce cell death in *N. benthamiana* whereas no cell death was triggered by
607 the expression of the inactive mutant StMAP3K β 2 (KD)^{Lys430Arg} or the empty vector
608 control. (B) The cell death triggered by StMAP3K β 2 and its active kinase domain is
609 suppressed by co-expression with Pi22926, but not EV control. Images taken under
610 UV light at 7 days. (C) Graph shows a significant increase in percentage of cell death
611 compared to EV control and inactive mutant KD (ANOVA, $p < 0.001$, 3 reps, $n = 72$). (D)
612 Graph shows that transient overexpression of Pi22926 can significantly suppress the
613 cell death (ANOVA, $p < 0.001$, 3 reps, $n = 72$) induced by StMAP3K β 2 and its active KD
614 compared to EV control. Lowercase letters on graphs denote statistically significant
615 groups. Error bars represent \pm SE.

616

617 **Figure 8. MEK2 and SIPK act downstream of StMAP3K β 2.** (A) *N. benthamiana*
618 plants were infected with TRV:GFP only or were silenced for the indicated MAP2Ks
619 (*MEK1* or *MEK2*) and MAPK (*SIPK*, *WIPK* or *NTF6*) genes. StMAP3K β 2 kinase
620 domain (KD) or inactive (KD mutant) were expressed in the leaves to measure cell
621 death. Photos were taken under UV light at 7 days. (B) and (C) Graph showing a
622 significant suppression of cell death triggered by StMAP3K ϵ (KD) or StMAP3K β 2(KD) in
623 TRV2:MEK2 and TRV2:SIPK plants compared to the TRV2:GFP control (ANOVA,
624 $p < 0.001$, 3 reps, $n \geq 155$). Error bars represent \pm SE.

625

626 **Figure 9. Pi22926 suppresses cell death triggered by StMAP3K β 2 whereas**
627 **PexRD2 suppresses StMAP3K ϵ -induced cell death.** (A) and (C) Images showing
628 StMAP3K β 2 (KD) and StMAP3K ϵ (KD) cell death at 7 days, following co-expression
629 with indicated effectors. (B) and (D) Graphs showing percentage of inoculation sites

630 developing cell death at 7 days after co-expression of StMAP3K β 2(KD) or
631 StMAP3K ϵ (KD) with indicated effectors. A significant decrease of cell death
632 percentage was observed when Pi22926 was co-expressed with StMAP3K β 2(KD) or
633 when PexRD2 was co-expressed with StMAP3K ϵ (KD), compared to co-expression
634 with other effectors and the EV control (ANOVA, $p < 0.001$, 4 reps, $n = 73$). Lowercase
635 letters on graphs denote statistically significant groups. Error bars represent \pm SE. (E)
636 Graph shows no significant decrease in mean percentage of cell death induced by
637 StMAP3K ϵ in TRV2:NbMAP3K β 2-3' and TRV2:NbMAP3K β 2-5' plants compared to
638 the TRV2-GFP control (7 days) (ANOVA, $p < 0.001$, 4 reps, $n = 92$) and (F) Graph
639 shows that VIGS of MAP3K ϵ by TRV2:NbMAP3K ϵ -3' and TRV2:NbMAP3K ϵ -5' had
640 no significant effect on StMAP3K β 2-induced cell death compared to the TRV:GFP
641 control (7 days). (ANOVA, $p < 0.001$, 4 reps, $n = 132$). Error bars represent \pm SE.

642

643 **Figure 10. Model of how PexRD2 and Pi22926 suppress two parallel MAPK**
644 **signalling pathways triggered by Avr4/Cf4 or AvrPto/Pto.** Schematic diagram
645 illustrating *P. infestans* delivering PexRD2 and Pi22926 inside the host cell during
646 infection. The cell death following recognition of the *C. fulvum* effector Avr4 by Cf4
647 and the *P. syringe* effector AvrPto mediated by Pto/Prf are dependent on MAPKKK ϵ
648 or MAP3K β 2 is suppressed respectively by the presence of PexRD2 or Pi22926.
649 PexRD2 or Pi22926 specifically interact with MAPKKK ϵ or MAP3K β 2 respectively. *In*
650 *planta*, MAPKKK ϵ and MAP3K β 2 confer enhanced resistance against *P. infestans*
651 likely due to recognition of an unidentified PAMP by a PRR or recognition of an
652 effector/avirulence protein (AVR) by an R protein as proposed by King et al. (2014).

653

654 References

655 Ah Fong AMV, Kim KS, Judelson HS (2017) RNA-seq of life stages of the oomycete
656 *Phytophthora infestans* reveals dynamic changes in metabolic, signal

657 transduction, and pathogenesis genes and a major role for calcium signaling in
658 development. *BMC Genomics* 18: 198.

659 Anderson RG, Deb D, Fedkenheuer K, McDowell JM (2015). Recent Progress in
660 RXLR Effector Research. *Mol Plant Microbe Interact* 28, 1063-1072.

661 Armstrong MR, Whisson SC, Pritchard L, Bos JI, Venter E, Avrova AO, Rehmany AP,
662 Böhme U, Brooks K, Cherevach I, Hamlin N, White B, Fraser A, Lord A, Quail MA,
663 Churcher C, Hall N, Berriman M, Huang S, Kamoun S, Beynon JL, Birch PR
664 (2005) An ancestral oomycete locus contains late blight avirulence gene *Avr3a*,
665 encoding a protein that is recognized in the host cytoplasm. *Proc Natl Acad Sci*
666 *USA* 102: 7766-7771.

667 Asai S, Ohta K, Yoshioka H (2008) MAPK signaling regulates nitric oxide and
668 NADPH oxidase-dependent oxidative bursts in *Nicotiana benthamiana*. *Plant Cell*
669 20: 1390-406.

670 Bi G, Zhou JM (2017) MAP kinase signaling pathways: a hub of plant-microbe
671 interactions. *Cell Host and Microbe* 21: 270-273.

672 Bi G, Zhou Z, Wang W, Li L, Rao S, Wu Y, Zhang X, Menke FLH, Chen S, Zhou J-M
673 (2018) Receptor-like cytoplasmic kinases directly link pattern recognition
674 receptors to the activation of mitogen-activated protein kinase cascades. *Plant*
675 *Cell* 30: 1543-1561.

676 Block A, Alfano JR (2011) Plant targets for *Pseudomonas syringae* type III effectors:
677 virulence targets or guarded decoys? *Curr Opin Microbiol.* 14: 39-46.

678 Bos JI, Armstrong MR, Gilroy EM, Boevink PC, Hein I, Taylor RM, Tian Z, Engelhardt
679 S, Vetukuri RR, Harrower B, Dixelius C, Bryan G, Sadanandom A, Whisson SC,
680 Kamoun S, Birch PR (2010) *Phytophthora infestans* effector AVR3a is essential
681 for virulence and manipulates plant immunity by stabilizing host E3 ligase CMPG1.
682 *Proc Natl Acad Sci USA* 107: 9909-9914.

683 Chisholm ST, Coaker G, Day B, Staskawicz BJ (2006) Host–microbe interactions:

684 shaping the evolution of the plant immune response. *Cell* 124: 803-814.

685 Colcombet J, Hirt H (2008) Arabidopsis MAPKs: a complex signalling network
686 involved in multiple biological processes. *Biochemical J.* 413: 217-226.

687 Cooke DE, Cano LM, Raffaele S, Bain RA, Cooke LR, Etherington GJ, Deahl KL,
688 Farrer RA, Gilroy EM, Goss EM, Grünwald NJ, Hein I, MacLean D, McNicol JW,
689 Randall E, Oliva RF, Pel MA, Shaw DS, Squires JN, Taylor MC, Vleeshouwers
690 VG, Birch PR, Lees AK, Kamoun S (2012) Genome analyses of an aggressive
691 and invasive lineage of the Irish potato famine pathogen. *PLoS Pathog.* 8:
692 e1002940.

693 Couto D, Zipfel C (2016) Regulation of pattern recognition receptor signalling in
694 plants. *Nat Rev Immunol.* 16: 537-552.

695 Cui H, Wang Y, Xue L, Chu J, Yan C, Fu J, Chen M, Innes RW, Zhou JM (2010)
696 *Pseudomonas syringae* effector protein AvrB perturbs Arabidopsis hormone
697 signalling by activating MAP kinase 4. *Cell Host Microbe* 7: 164-175.

698 del Pozo O, Pedley KF, Martin GB (2004) MAPKKK α is a positive regulator of
699 cell death associated with both plant immunity and disease. *EMBO J.* 23:
700 3072-3082.

701 Deslandes L, Rivas S (2012) Catch me if you can: bacterial effectors and plant
702 targets. *Trends Plant Sci.* 17: 644-655.

703 Dodds PN, Rathjen JP (2010) Plant immunity: Towards an integrated view of
704 plant-pathogen interactions. *Nat Rev Genet.* 11: 539-548.

705 Dou D, Kale SD, Wang X, Jiang RH, Bruce NA, Arredondo FD, Zhang X, Tyler BM.
706 (2008) RXLR-mediated entry of *Phytophthora sojae* effector Avr1b into soybean
707 cells does not require pathogen-encoded machinery. *Plant Cell* 20: 1930-1947.

708 Dou D, Zhou JM (2012) Phytopathogen effectors subverting host immunity: different
709 foes, similar battleground. *Cell Host Microbe* 12: 484-495.

710 Ekengren SK, Liu Y, Schiff M, Dinesh-Kumar SP, Martin GB (2003) Two MAPK

711 cascades, NPR1, and TGA transcription factors play a role in Pto-mediated
712 disease resistance in tomato. *Plant J.* 36: 905-917.

713 Frye CA, Tang D, Innes RW (2001) Negative regulation of defense responses in
714 plants by a conserved MAPKK kinase. *Proc Natl Acad Sci USA* 98: 373-378.

715 Gao M, Liu J, Bi D, Zhang Z, Cheng F, Chen S, Zhang Y (2008) MEKK1,
716 MKK1/MKK2 and MPK4 function together in a mitogen-activated protein kinase
717 cascade to regulate innate immunity in plants. *Cell Res.* 18: 1190-1198.

718 Haas BJ, Kamoun S, Zody MC et al. (2009) Genome sequence and analysis of the
719 Irish potato famine pathogen *Phytophthora infestans*. *Nature* 461: 393-398.

720 Hashimoto M, Komatsu K, Maejima K, Okano Y, Shiraishi T, Ishikawa K, Takinami Y,
721 Yamaji Y, Namba S (2012) Identification of three MAPKKKs forming a linear
722 signaling pathway leading to programmed cell death in *Nicotiana benthamiana*.
723 *BMC Plant Biol.* 12: 103.

724 Jin H, Axtell MJ, Dahlbeck D, Ekwenna O, Zhang S, Staskawicz B, Baker B (2002)
725 NPK1, an MEKK1-like mitogen-activated protein kinase kinase kinase, regulates
726 innate immunity and development in plants. *Dev Cell* 3: 291-297.

727 Jones J, Dangl J (2006) The plant immune system. *Nature* 444: 323-329.

728 Kamoun S, Furzer O, Jones JD, Judelson HS, Ali GS., et al. (2015) The top 10
729 oomycete pathogens in molecular plant pathology. *Mol Plant Pathol.* 16: 413-434.

730 Kamoun S, van West, PVleeshouwers VG, de Groot KE, Govers F (1998)
731 Resistance of *Nicotiana benthamiana* to *Phytophthora infestans* is mediated by
732 the recognition of the elicitor protein INF1. *Plant Cell* 10: 1413-1426.

733 King SR, McLellan H, Boevink PC, Armstrong MR, Bukharova T, Sukarta O, Win J,
734 Kamoun S, Birch PR, Banfield MJ (2014) *Phytophthora infestans* RXLR effector
735 PexRD2 interacts with host MAPKKKε to suppress plant immune signaling. *Plant*
736 *Cell* 26: 1345-1359.

737 Liu Y, Schiff M, Marathe R, Dinesh-Kumar SP (2002) Tobacco Rar1, EDS1 and

738 NPR1/NIM1 like genes are required for N-mediated resistance to tobacco mosaic
739 virus. *Plant J.* 30: 415-429.

740 MAPK Group (2002) Mitogen-activated protein kinase cascades in plants: a new
741 nomenclature. *Trends Plant Sci.* 7: 301-308.

742 McLellan H, Boevink PC, Armstrong MR, Pritchard L, Gomez S, Morales J, Whisson
743 SC, Beynon JL, Birch PR (2013) An RxLR effector from *Phytophthora infestans*
744 prevents re-localisation of two plant NAC transcription factors from the
745 endoplasmic reticulum to the nucleus. *PLoS Pathog.* 9: e1003670.

746 Melech-Bonfil S, and Sessa G (2010) Tomato MAPKKKε is a positive regulator of
747 cell-death signaling networks associated with plant immunity. *Plant J.* 64:
748 379-391.

749 Moffett P, Farnham G, Peart J, Baulcombe DC (2002) Interaction between domains
750 of a plant NBS-LRR protein in disease resistance-related cell death. *EMBO J.* 21:
751 4511-4519

752 Mukhtar MS, Carvunis A-R, Dreze M, Epple P, Steinbrenner J., et al. (2011)
753 Independently evolved virulence effectors converge onto hubs in a plant immune
754 system network. *Science* 333: 596-600.

755 Murphy F, He Q, Armstrong M, Giuliani LM, Boevink PC, Zhang W, Tian Z, Birch RR,
756 Gilroy EM (2018) Potato MAP3K StVIK is required for *Phytophthora infestans*
757 RXLR Effector Pi17316 to promote disease. *Plant Physiol.* 177(1): 398-410.

758 Pedley KF, Martin GB (2005) Role of mitogen-activated protein kinases in plant
759 immunity. *Curr Opin Plant Biol.* 8: 541-547.

760 Pitzschke A, Schikora A, Hirt H (2009) MAPK cascade signalling networks in plant
761 defence. *Curr Opin Plant Biol.* 12: 421-426.

762 Suarez-Rodriguez MC, Adams-Phillips L, Liu Y, Wang H, Su SH, Jester PJ, Zhang S,
763 Bent AF, Krysan PJ (2007) MEKK1 is required for flg22-induced MPK4 activation
764 in Arabidopsis plants. *Plant Physiol.* 143: 661-669.

-
- 765 Sun T, Nitta Y, Zhang Q, Wu D, Tian H, Lee JS, Zhang Y (2018) Antagonistic
766 interactions between two MAP kinase cascades in plant development and
767 immune signaling. *EMBO Reports* 19: e45324.
- 768 Toruño TY, Stergiopoulos I, Coaker G (2016) Plant-pathogen effectors: cellular
769 probes interfering with plant defenses in special and temporal manners. *Ann Rev*
770 *Phytopathol* 54: 419-441. Wang S, Boevink PC, Welsh L, Zhang R, Whisson SC,
771 Birch PRJ (2017) Delivery of cytoplasmic and apoplastic effectors from
772 *Phytophthora infestans* haustoria by distinct secretion pathways. *New Phytol.* 216:
773 205-215.
- 774 Wang S, McLellan H, Bukharova T, He Q, Murphy F, et al (2018b) *Phytophthora*
775 *infestans* RXLR effectors act in concert at diverse subcellular localisations to
776 enhance host colonization. *J Exp Bot* 70: 343-356.
- 777 Wang S, Welsh L, Thorpe P, Whisson SC, Boevink PC, Birch PRJ. (2018a) The
778 *Phytophthora infestans* haustorium is a site for secretion of diverse classes of
779 infection associated proteins. *mBio* 9: e01216-18.
- 780 Wang X, Boevink P, McLellan H, Armstrong M, Bukharova T, Qin Z, Birch PR (2015)
781 A Host KH RNA-Binding protein is a susceptibility factor targeted by an RXLR
782 effector to promote Late blight disease. *Mol Plant* 8: 1385-1395.
- 783 Weßling R, Epple P, Altmann S, He Y, Yang L, et al. (2014) Convergent targeting of
784 a common host protein network by pathogen effectors from three kingdoms of life.
785 *Cell Host Microbe* 16: 364-375.
- 786 Whisson SC, Boevink PC, Moleleki L, Avrova AO, Morales JG, Gilroy EM, Armstrong
787 MR, Grouffaud S, West PV, Chapman S et al. (2007) A translocation signal for
788 delivery of oomycete effector proteins into host plant cells. *Nature* **450**: 115-118.
- 789 Whisson SC, Boevink PC, Wang S, Birch PR (2016) The cell biology of late blight
790 disease. *Curr Opin Microbiol.* 34: 127-135.
- 791 Yang L, McLellan H, Naqvi S, He Q, Boevink PC, Armstrong M, Giuliani LM, Zhang

-
- 792 W, Tian Z, Zhan J, Gilroy EM, Birch PR (2016) Potato NPH3/RPT2-Like protein
793 StNRL1, targeted by a *Phytophthora infestans* RXLR effector, is a susceptibility
794 factor. *Plant Physiol.*171: 645-657.
- 795 Yin JL, Gu B, Huang GY, Tian Y, Quan JL, Lindqvist-Kreuze H, Shan WX (2017)
796 Conserved RXLR effector genes of *Phytophthora infestans* expressed at the early
797 stage of potato infection are suppressive to host defense. *Front Plant Sci.* 8:
798 2155.
- 799 Zheng X, McLellan H, Fraiture M, Liu X, Boevink PC, Gilroy EM, Ying C, Kandel K,
800 Sessa G, Birch PR, Brunner F (2014) Functionally redundant RXLR effectors from
801 *Phytophthora infestans* act at different steps to suppress early flg22-triggered
802 immunity. *PLoS Pathog.* 10(4): e1004057.

Figure 1

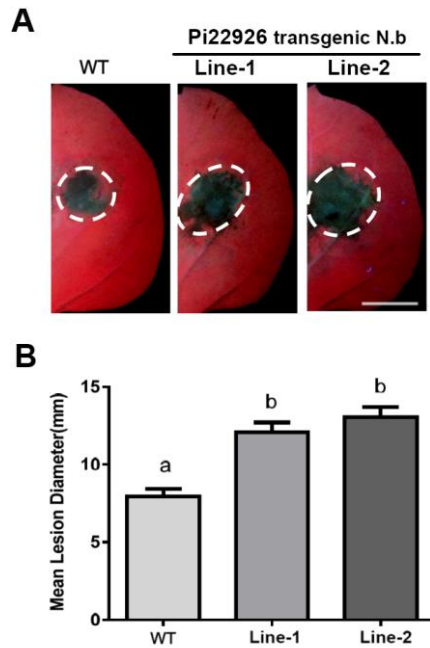


Figure 1. The RXLR effector Pi22926 enhances *P. infestans* colonization of *N. benthamiana* leaves. (A) Representative images taken under UV light at 5 days after inoculation show that transgenic lines overexpressing GFP-Pi22926 enhance pathogen colonization compared to the untransformed *N. benthamiana* control. Scale bar represents 1 cm. (B) Graph shows a significant increase in *P. infestans* lesions in transgenic lines overexpressing GFP-Pi22926 compared to wild type *N. benthamiana* control (ANOVA, $p < 0.001$, 3 reps, $n = 120$). Lowercase letters on graphs denote statistically significant groups. Error bars represent \pm SE.

Figure 2

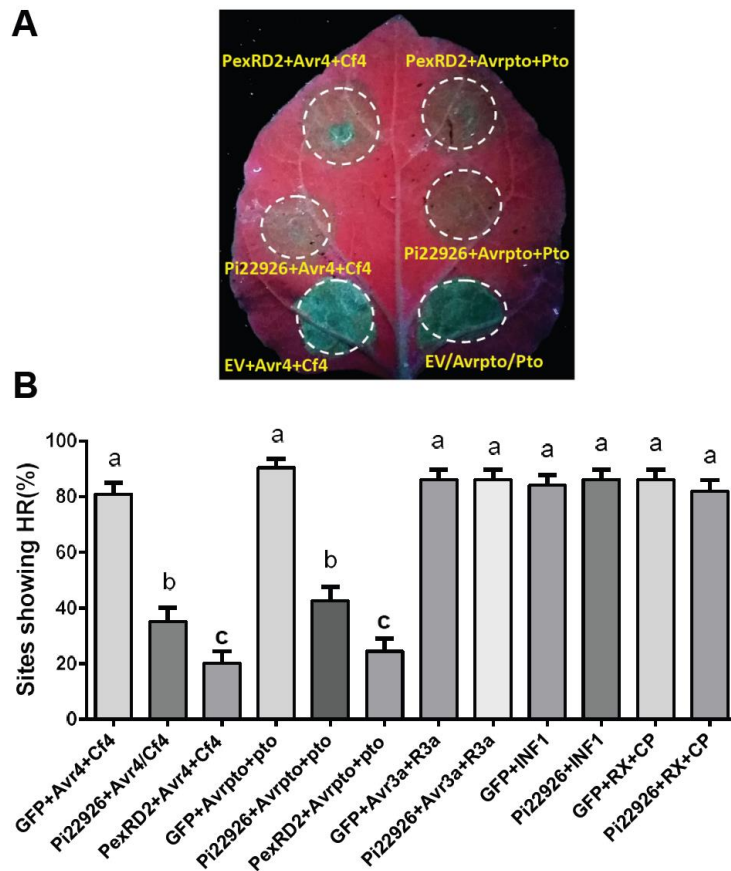


Figure 2. Pi22926 specifically suppresses Avr4/Cf4 and AvrPto/Pto induced cell death. (A) Representative leaf image taken under UV light at 5 days showing Avr4/Cf4 and AvrPto/Pto cell death with EV, Pi22926 and PexRD2 positive control. (B) Graph showing Pi22926 and PexRD2 expression lead to a significant decrease ($p < 0.001$, 3 reps, $n = 94$) in cell death percentage triggered by Avr4/Cf4 and AvrPto/Pto. Lowercase letters on graphs denote statistically significant groups by one-way ANOVA, with pairwise comparisons performed with the Holm-Sidak method. Error bars represent \pm SE.

Figure 3

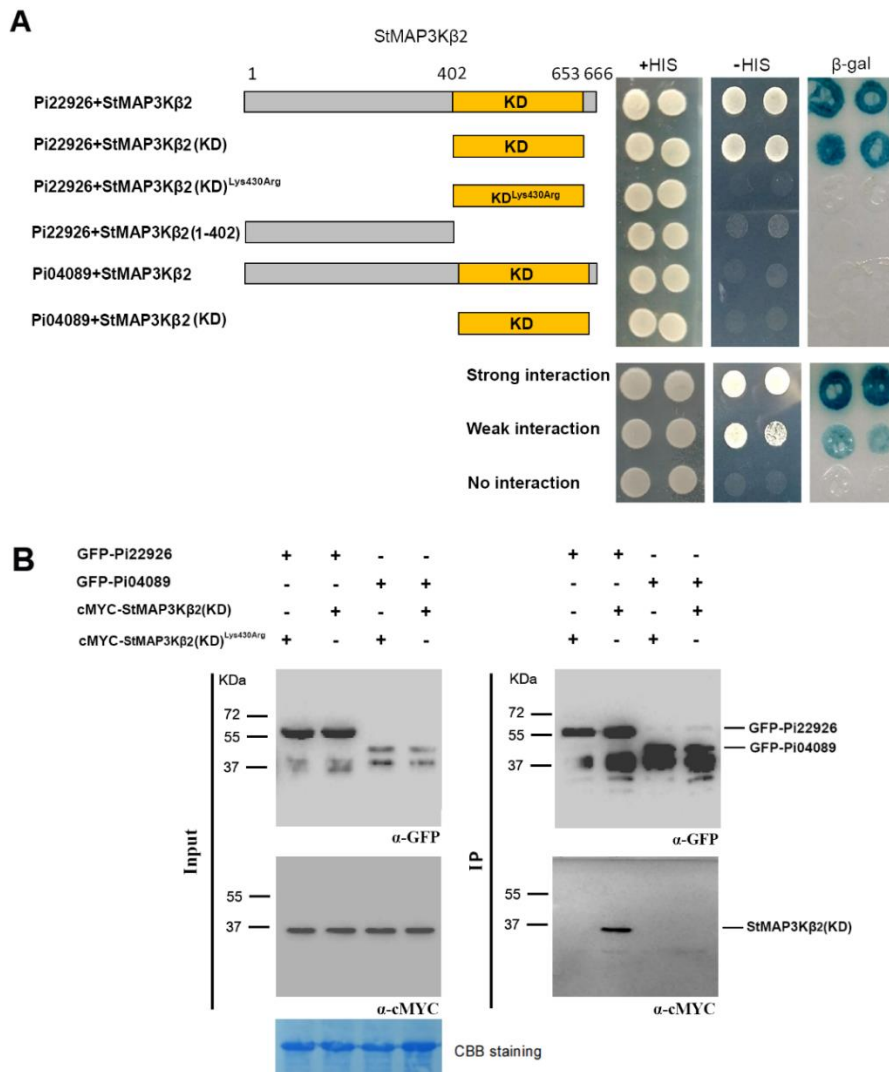


Figure 3. Pi22926 interacts with the kinase domain of StMAP3Kβ2 in Y2H and immunoprecipitation assays. (A) Yeast co-expressing Pi22926 with StMAP3Kβ2 and its kinase domain grow on –histidine (-HIS) medium and had β-galactosidase (β-gal) activity, whereas those co-expressed with the inactive mutant kinase domain StMAP3Kβ2(KD)^{Lys430Arg} or the control Pi04089 did not. (B) Co-immunoprecipitation from leaf extracts using GFP-trap (GFP IP) confirmed that cMyc tagged StMAP3Kβ2 KD specifically interacted with GFP-Pi22926 and not with Pi04089. Expression of constructs is indicated by +. Protein size markers are indicated in kDa, and protein loading is indicated by Coomassie brilliant blue (CBB) staining.



Figure 4

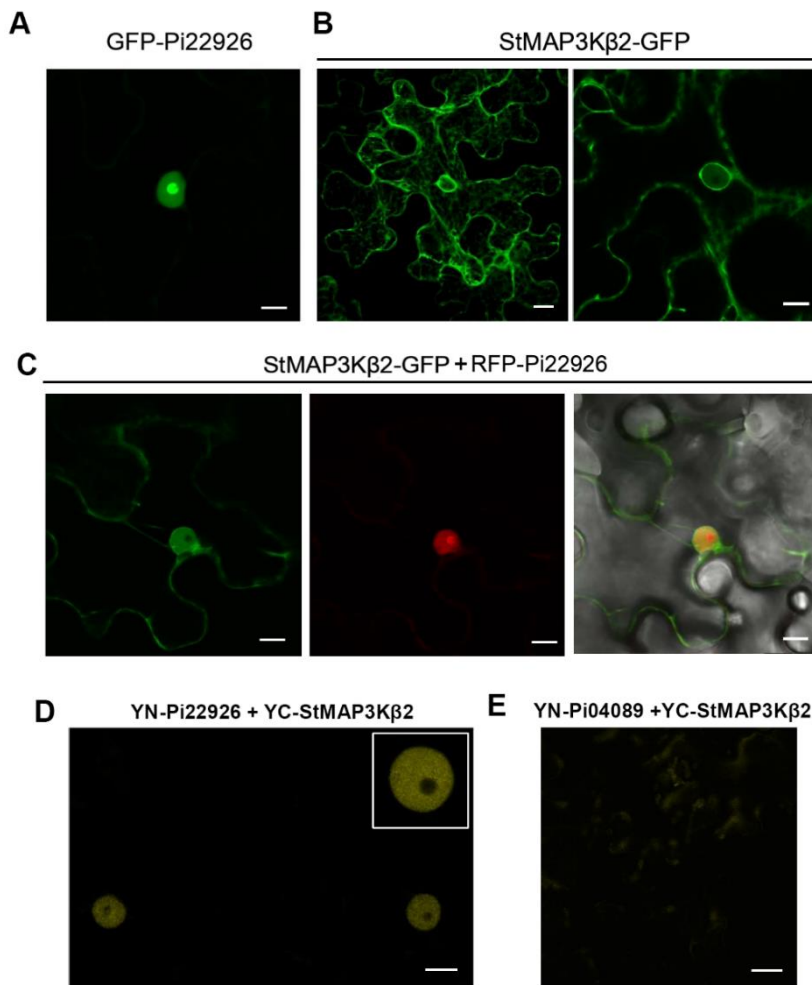


Figure 4. Pi22926 interacts with StMAP3Kβ2 in nucleoplasm. (A) Confocal images show that GFP-Pi22926 is localized in the nucleoplasm and nucleolus. (B) StMAP3Kβ2-GFP is localized in the cytoplasm and nucleoplasm. For images of StMAP3Kβ2-GFP, the left one is a Z-stack, whereas the right one with higher magnification is a single optical section from the stack. (C) Images show transient co-expression of StMAP3Kβ2-GFP with RFP-Pi22926. (D) Images show transient co-expression of YC-StMAP3Kβ2 with YN-Pi22926. Inset image is a nucleus at higher magnification. (E) Images show transient co-expression of YC-StMAP3Kβ2 with YN-Pi04089. Scale bars represent 10 μm. OD₆₀₀ of Agrobacteria suspension for GFP and RFP constructs is 0.1 and 0.03 for split YFP.

Figure 5

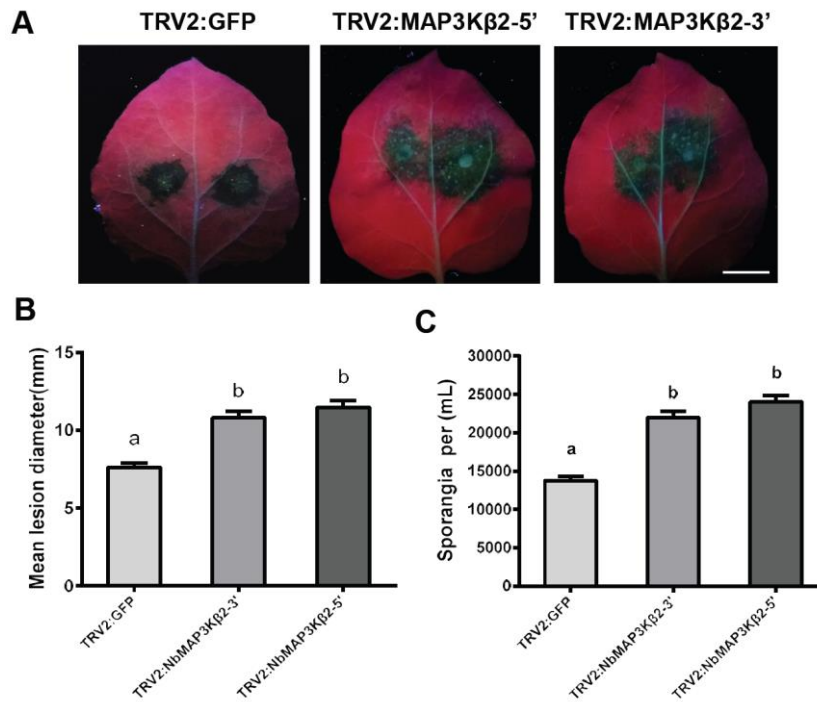


Figure 5. Silencing of *NbMAP3Kβ2* enhances *P. infestans* leaf colonization. (A) Images taken at 7 days after sporangia inoculation indicate more pathogen colonization on TRV:NbMAP3Kβ2 plants compared to the TRV:GFP control. Scale bar represents 1 cm. (B) Graph shows a significant increase (ANOVA, $p < 0.001$, 3 reps, $n = 120$) in *P. infestans* lesion diameter in plants expressing TRV:NbMAP3Kβ2-3' and TRV:NbMAP3Kβ2-5', compared with a TRV-GFP control. (C) Graph shows an increase in the average numbers of sporangia mL^{-1} collected from infected leaves expressing TRV:NbMAP3Kβ2-3' and TRV:NbMAP3Kβ2-5', compared with a TRV:GFP control (ANOVA, $p < 0.001$, 3 reps, $n = 120$). Lowercase letters on graphs denote statistically significant groups. Error bars represent \pm SE.

Figure 6

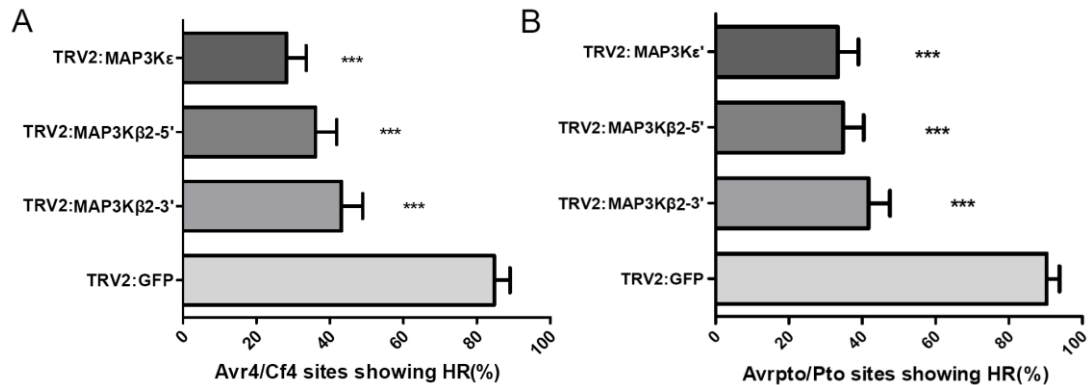


Figure 6. Cell death induced by Avr4/Cf4 and Avrpto/Pto is dependent on MAP3Kε and NbMAP3Kβ2. (A) Graph showing a significant suppression of cell death (ANOVA, $p < 0.001$, 3 reps, $n = 72$) induced by Avr4/Cf4 in *NbMAP3Kβ2* silenced plants, and in positive control *NbMAP3Kε* silenced plants, compared to TRV2:GFP control. (B) Graph showing a significant decrease of cell death (ANOVA, $p < 0.001$, 3 reps, $n = 72$) triggered by Avrpto/Pto in *NbMAP3Kβ2* silenced plants, and positive control *NbMAP3Kε* silenced plants, compared to TRV2:GFP control. Error bars represent \pm SE. Cell death numbers were counted at 6 days. Stars indicate significant difference to the TRV:GFP control.

Figure 7

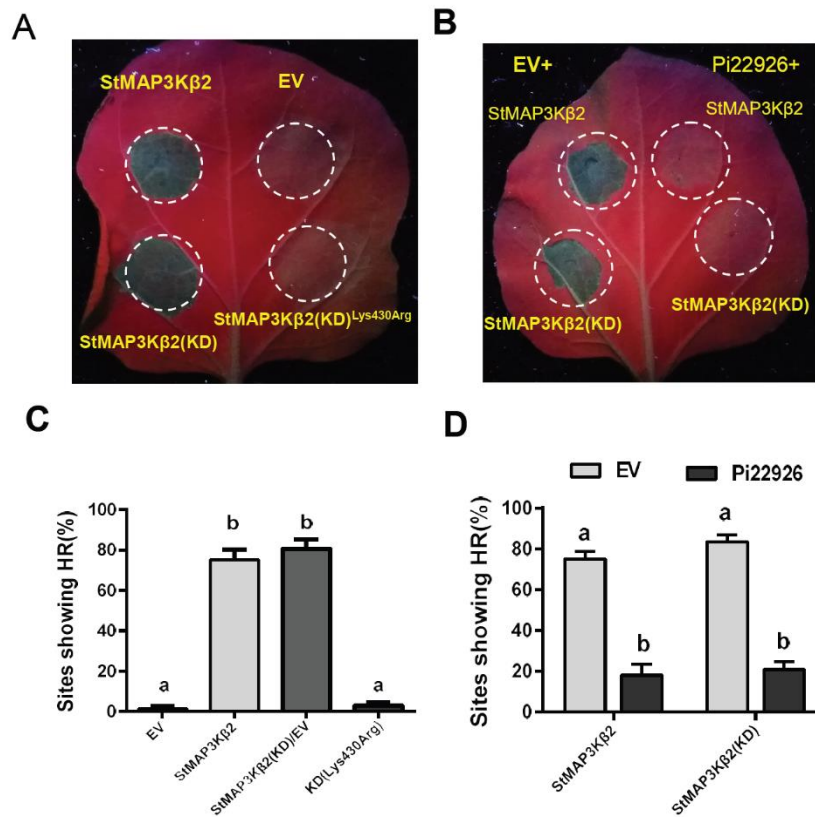


Figure 7. Overexpression of StMAP3Kβ2 or its kinase domain induces cell death that is suppressed by Pi22926. (A) Images taken under UV light at 7 days after inoculation showing that transient overexpression of StMAP3Kβ2 and its kinase domain induce cell death in *N. benthamiana* whereas no cell death was triggered by the expression of the inactive mutant StMAP3Kβ2 (KD)^{Lys430Arg} or the empty vector control. (B) The cell death triggered by StMAP3Kβ2 and its active kinase domain is suppressed by co-expression with Pi22926, but not EV control. Images taken under UV light at 7 days. (C) Graph shows a significant increase in percentage of cell death compared to EV control and inactive mutant KD (ANOVA, $p < 0.001$, 3 reps, $n = 72$). (D) Graph shows that transient overexpression of Pi22926 can significantly suppress the cell death (ANOVA, $p < 0.001$, 3 reps, $n = 72$) induced by StMAP3Kβ2 and its active KD compared to EV control. Lowercase letters on graphs denote statistically significant groups. Error bars represent \pm SE.

Figure 8

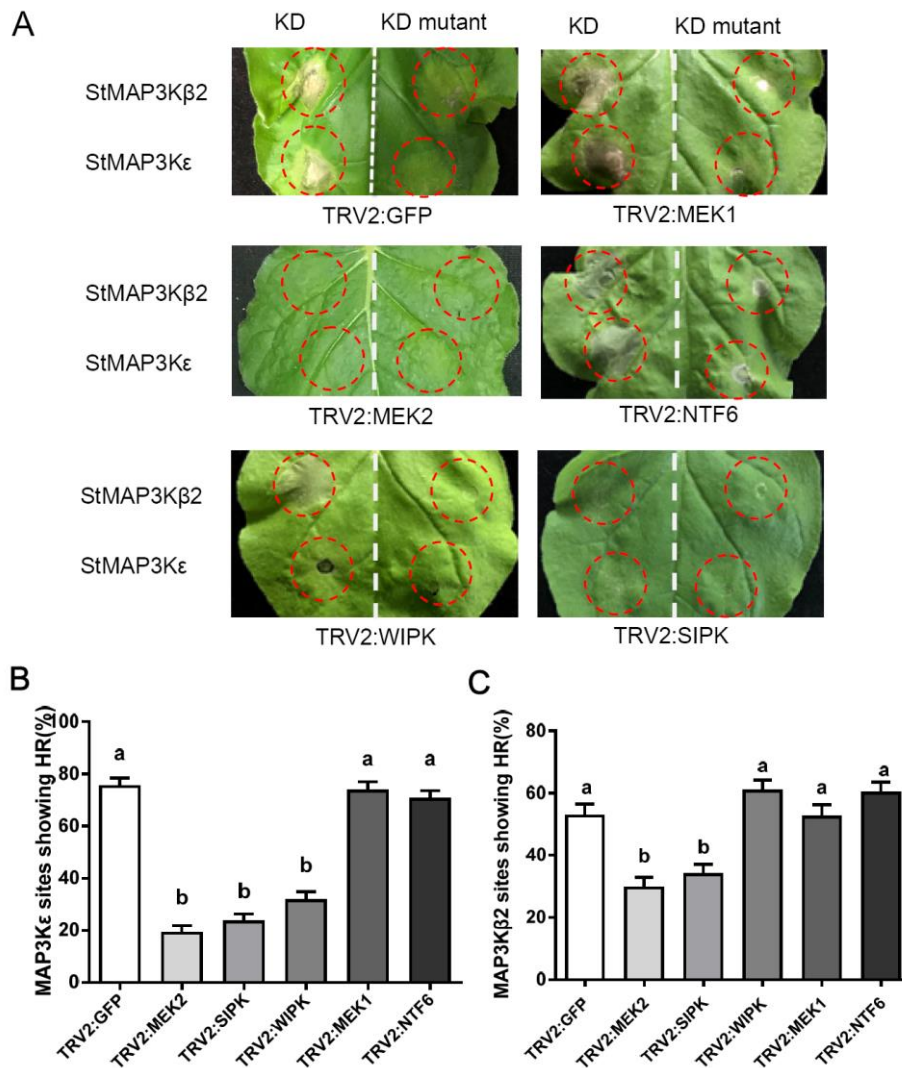


Figure 8. MEK2 and SIPK act downstream of StMAP3Kβ2. (A) *N. benthamiana* plants were infected with TRV:GFP only or were silenced for the indicated MAP2Ks (*MEK1* or *MEK2*) and MAPK (*SIPK*, *WIPK* or *NTF6*) genes. StMAP3Kβ2 kinase domain (KD) or inactive (KD mutant) were expressed in the leaves to measure cell death. Photos were taken under UV light at 7 days. (B) and (C) Graph showing a significant suppression of cell death triggered by StMAP3Kε(KD) or StMAP3Kβ2(KD) in TRV2:MEK2 and TRV2:SIPK plants compared to the TRV2:GFP control (ANOVA, $p < 0.001$, 3 reps, $n \geq 155$). Error bars represent \pm SE.

Figure 9

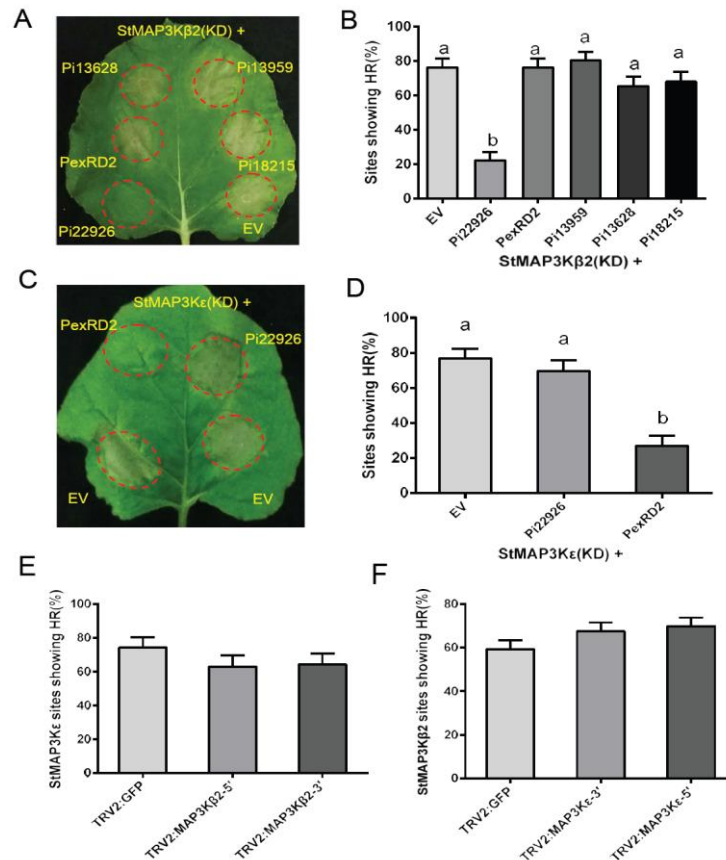


Figure 9. Pi22926 suppresses cell death triggered by StMAP3Kβ2 whereas PexRD2 suppresses StMAP3Kε-induced cell death. (A) and (C) Images showing StMAP3Kβ2 (KD) and StMAP3Kε(KD) cell death at 7 days, following co-expression with indicated effectors. (B) and (D) Graphs showing percentage of inoculation sites developing cell death at 7 days after co-expression of StMAP3Kβ2(KD) or StMAP3Kε(KD) with indicated effectors. A significant decrease of cell death percentage was observed when Pi22926 was co-expressed with StMAP3Kβ2(KD) or when PexRD2 was co-expressed with StMAP3Kε(KD), compared to co-expression with other effectors and the EV control (ANOVA, $p < 0.001$, 4 reps, $n = 73$). Lowercase letters on graphs denote statistically significant groups. Error bars represent \pm SE. (E) Graph shows no significant decrease in mean percentage of cell death induced by StMAP3Kε in TRV2:NbMAP3Kβ2-3' and TRV2:NbMAP3Kβ2-5' plants compared to the TRV2-GFP control (7 days) (ANOVA, $p < 0.001$, 4 reps, $n = 92$) and (F) Graph shows that VIGS of MAP3Kε by TRV2:NbMAP3Kε-3' and TRV2-NbMAP3Kε-5' had no significant effect on StMAP3Kβ2-induced cell death compared to the TRV:GFP control (7 days). (ANOVA, $p < 0.001$, 4 reps, $n = 132$). Error bars represent \pm SE.

Figure 10

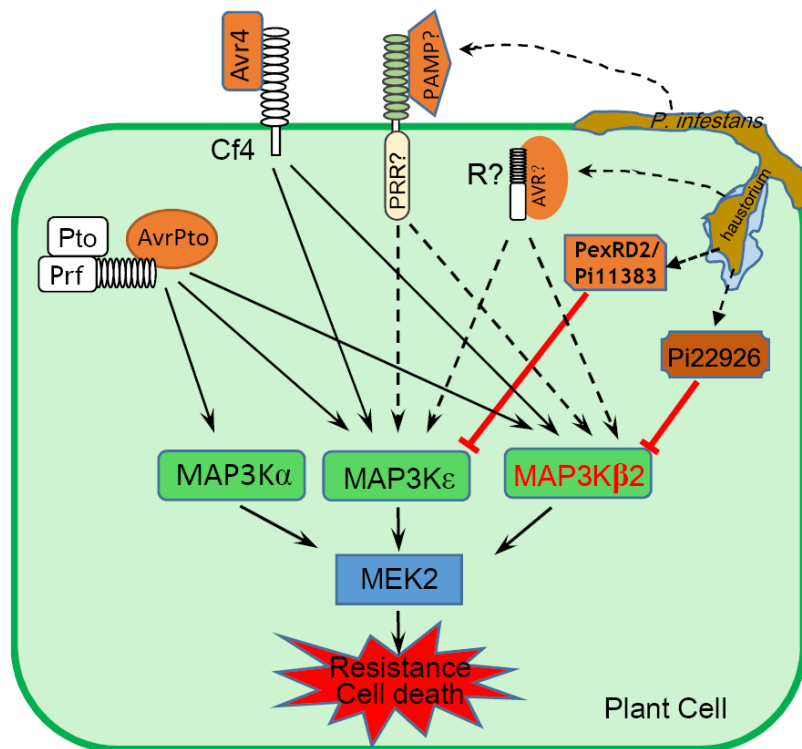


Figure 10. Model of how PexRD2 and Pi22926 suppress two parallel MAPK signalling pathways triggered by Avr4/Cf4 or AvrPto/Pto. Schematic diagram illustrating *P. infestans* delivering PexRD2 and Pi22926 inside the host cell during infection. The cell death following recognition of the *C. fulvum* effector Avr4 by Cf4 and the *P. syringe* effector AvrPto mediated by Pto/Prf are dependent on MAPKKE or MAP3Kβ2 is suppressed respectively by the presence of PexRD2 or Pi22926. PexRD2 or Pi22926 specifically interact with MAPKKE or MAP3Kβ2 respectively. *In planta*, MAPKKE and MAP3Kβ2 confer enhanced resistance against *P. infestans* likely due to recognition of an unidentified PAMP by a PRR or recognition of an effector/avirulence protein (AVR) by an R protein as proposed by King et al. (2014).

Parsed Citations

Ah Fong AMV, Kim KS, Judelson HS (2017) RNA-seq of life stages of the oomycete *Phytophthora infestans* reveals dynamic changes in metabolic, signal transduction, and pathogenesis genes and a major role for calcium signaling in development. *BMC Genomics* 18: 198.

Pubmed: [Author and Title](#)

Google Scholar: [Author Only Title Only Author and Title](#)

Anderson RG, Deb D, Fedkenheuer K, McDowell JM (2015). Recent Progress in RXLR Effector Research. *Mol Plant Microbe Interact* 28, 1063-1072.

Pubmed: [Author and Title](#)

Google Scholar: [Author Only Title Only Author and Title](#)

Armstrong MR, Whisson SC, Pritchard L, Bos JI, Venter E, Avrova AO, Rehmany AP, Böhme U, Brooks K, Cherevach I, Hamlin N, White B, Fraser A, Lord A, Quail MA, Churcher C, Hall N, Berriman M, Huang S, Kamoun S, Beynon JL, Birch PR (2005) An ancestral oomycete locus contains late blight avirulence gene *Avr3a*, encoding a protein that is recognized in the host cytoplasm. *Proc Natl Acad Sci USA* 102: 7766-7771.

Pubmed: [Author and Title](#)

Google Scholar: [Author Only Title Only Author and Title](#)

Asai S, Ohta K, Yoshioka H (2008) MAPK signaling regulates nitric oxide and NADPH oxidase-dependent oxidative bursts in *Nicotiana benthamiana*. *Plant Cell* 20: 1390-406.

Pubmed: [Author and Title](#)

Google Scholar: [Author Only Title Only Author and Title](#)

Bi G, Zhou JM (2017) MAP kinase signaling pathways: a hub of plant-microbe interactions. *Cell Host and Microbe* 21: 270-273.

Pubmed: [Author and Title](#)

Google Scholar: [Author Only Title Only Author and Title](#)

Bi G, Zhou Z, Wang W, Li L, Rao S, Wu Y, Zhang X, Menke FLH, Chen S, Zhou J-M (2018) Receptor-like cytoplasmic kinases directly link pattern recognition receptors to the activation of mitogen-activated protein kinase cascades. *Plant Cell* 30: 1543-1561.

Pubmed: [Author and Title](#)

Google Scholar: [Author Only Title Only Author and Title](#)

Block A, Alfano JR (2011) Plant targets for *Pseudomonas syringae* type III effectors: virulence targets or guarded decoys? *Curr Opin Microbiol.* 14: 39-46.

Pubmed: [Author and Title](#)

Google Scholar: [Author Only Title Only Author and Title](#)

Bos JI, Armstrong MR, Gilroy EM, Boevink PC, Hein I, Taylor RM, Tian Z, Engelhardt S, Vetukuri RR, Harrower B, Dixelius C, Bryan G, Sadanandom A, Whisson SC, Kamoun S, Birch PR (2010) *Phytophthora infestans* effector AVR3a is essential for virulence and manipulates plant immunity by stabilizing host E3 ligase CMPG1. *Proc Natl Acad Sci USA* 107: 9909-9914.

Pubmed: [Author and Title](#)

Google Scholar: [Author Only Title Only Author and Title](#)

Chisholm ST, Coaker G, Day B, Staskawicz BJ (2006) Host-microbe interactions: shaping the evolution of the plant immune response. *Cell* 124: 803-814.

Pubmed: [Author and Title](#)

Google Scholar: [Author Only Title Only Author and Title](#)

Colcombet J, Hirt H (2008) Arabidopsis MAPKs: a complex signalling network involved in multiple biological processes. *Biochemical J.* 413: 217-226.

Pubmed: [Author and Title](#)

Google Scholar: [Author Only Title Only Author and Title](#)

Cooke DE, Cano LM, Raffaele S, Bain RA, Cooke LR, Etherington GJ, Deahl KL, Farrer RA, Gilroy EM, Goss EM, Grünwald NJ, Hein I, MacLean D, McNicol JW, Randall E, Oliva RF, Pei MA, Shaw DS, Squires JN, Taylor MC, Vleeshouwers VG, Birch PR, Lees AK, Kamoun S (2012) Genome analyses of an aggressive and invasive lineage of the Irish potato famine pathogen. *PLoS Pathog.* 8: e1002940.

Pubmed: [Author and Title](#)

Google Scholar: [Author Only Title Only Author and Title](#)

Couto D, Zipfel C (2016) Regulation of pattern recognition receptor signalling in plants. *Nat Rev Immunol.* 16: 537-552.

Pubmed: [Author and Title](#)

Google Scholar: [Author Only Title Only Author and Title](#)

Cui H, Wang Y, Xue L, Chu J, Yan C, Fu J, Chen M, Innes RW, Zhou JM (2010) *Pseudomonas syringae* effector protein AvrB perturbs Arabidopsis hormone signalling by activating MAP kinase 4. *Cell Host Microbe* 7: 164-175.

Pubmed: [Author and Title](#)

Google Scholar: [Author Only Title Only Author and Title](#)

del Pozo O, Pedley KF, Martin GB (2004) MAPKKK α is a positive regulator of cell death associated with both plant immunity and disease. *EMBO J.* 23: 3072-3082.

Pubmed: [Author and Title](#)

Google Scholar: [Author Only Title Only Author and Title](#)

Deslandes L, Rivas S (2012) Catch me if you can: bacterial effectors and plant targets. Trends Plant Sci. 17: 644-655.

Pubmed: [Author and Title](#)

Google Scholar: [Author Only](#) [Title Only](#) [Author and Title](#)

Dodds PN, Rathjen JP (2010) Plant immunity: Towards an integrated view of plant-pathogen interactions. Nat Rev Genet. 11: 539-548.

Pubmed: [Author and Title](#)

Google Scholar: [Author Only](#) [Title Only](#) [Author and Title](#)

Dou D, Kale SD, Wang X, Jiang RH, Bruce NA, Arredondo FD, Zhang X, Tyler BM. (2008) RXLR-mediated entry of *Phytophthora sojae* effector Avr1b into soybean cells does not require pathogen-encoded machinery. Plant Cell 20: 1930-1947.

Pubmed: [Author and Title](#)

Google Scholar: [Author Only](#) [Title Only](#) [Author and Title](#)

Dou D, Zhou JM (2012) Phytopathogen effectors subverting host immunity: different foes, similar battleground. Cell Host Microbe 12: 484-495.

Pubmed: [Author and Title](#)

Google Scholar: [Author Only](#) [Title Only](#) [Author and Title](#)

Ekengren SK, Liu Y, Schiff M, Dinesh-Kumar SP, Martin GB (2003) Two MAPK cascades, NPR1, and TGA transcription factors play a role in Pto-mediated disease resistance in tomato. Plant J. 36: 905-917.

Pubmed: [Author and Title](#)

Google Scholar: [Author Only](#) [Title Only](#) [Author and Title](#)

Frye CA, Tang D, Innes RW (2001) Negative regulation of defense responses in plants by a conserved MAPKK kinase. Proc Natl Acad Sci USA 98: 373-378.

Pubmed: [Author and Title](#)

Google Scholar: [Author Only](#) [Title Only](#) [Author and Title](#)

Gao M, Liu J, Bi D, Zhang Z, Cheng F, Chen S, Zhang Y (2008) MEKK1, MKK1/MKK2 and MPK4 function together in a mitogen-activated protein kinase cascade to regulate innate immunity in plants. Cell Res. 18: 1190-1198.

Pubmed: [Author and Title](#)

Google Scholar: [Author Only](#) [Title Only](#) [Author and Title](#)

Haas BJ, Kamoun S, Zody MC et al. (2009) Genome sequence and analysis of the Irish potato famine pathogen *Phytophthora infestans*. Nature 461: 393-398.

Pubmed: [Author and Title](#)

Google Scholar: [Author Only](#) [Title Only](#) [Author and Title](#)

Hashimoto M, Komatsu K, Maejima K, Okano Y, Shiraishi T, Ishikawa K, Takinami Y, Yamaji Y, Namba S (2012) Identification of three MAPKKs forming a linear signaling pathway leading to programmed cell death in *Nicotiana benthamiana*. BMC Plant Biol. 12: 103.

Pubmed: [Author and Title](#)

Google Scholar: [Author Only](#) [Title Only](#) [Author and Title](#)

Jin H, Axtell MJ, Dahlbeck D, Ekwenna O, Zhang S, Staskawicz B, Baker B (2002) NPK1, an MEKK1-like mitogen-activated protein kinase kinase kinase, regulates innate immunity and development in plants. Dev Cell 3: 291-297.

Pubmed: [Author and Title](#)

Google Scholar: [Author Only](#) [Title Only](#) [Author and Title](#)

Jones J, Dangl J (2006) The plant immune system. Nature 444: 323-329.

Pubmed: [Author and Title](#)

Google Scholar: [Author Only](#) [Title Only](#) [Author and Title](#)

Kamoun S, Furzer O, Jones JD, Judelson HS, Ali GS., et al. (2015) The top 10 oomycete pathogens in molecular plant pathology. Mol Plant Pathol. 16: 413-434.

Pubmed: [Author and Title](#)

Google Scholar: [Author Only](#) [Title Only](#) [Author and Title](#)

Kamoun S, van West, PMeeshouwers VG, de Groot KE, Govers F (1998) Resistance of *Nicotiana benthamiana* to *Phytophthora infestans* is mediated by the recognition of the elicitor protein INF1. Plant Cell 10: 1413-1426.

Pubmed: [Author and Title](#)

Google Scholar: [Author Only](#) [Title Only](#) [Author and Title](#)

King SR, McLellan H, Boevink PC, Armstrong MR, Bukharova T, Sukarta O, Win J, Kamoun S, Birch PR, Banfield MJ (2014) *Phytophthora infestans* RXLR effector PexRD2 interacts with host MAPKKKε to suppress plant immune signaling. Plant Cell 26: 1345-1359.

Pubmed: [Author and Title](#)

Google Scholar: [Author Only](#) [Title Only](#) [Author and Title](#)

Liu Y, Schiff M, Marathe R, Dinesh-Kumar SP (2002) Tobacco Rar1, EDS1 and NPR1/NIM1 like genes are required for N-mediated resistance to tobacco mosaic virus. Plant J. 30: 415-429.

Pubmed: [Author and Title](#)

Google Scholar: [Author Only](#) [Title Only](#) [Author and Title](#)

MAPK Group (2002) Mitogen-activated protein kinase cascades in plants: a new nomenclature. Trends Plant Sci. 7: 301-308.

Pubmed: [Author and Title](#)

Downloaded from on June 25, 2019 - Published by www.plantphysiol.org
Copyright © 2019 American Society of Plant Biologists. All rights reserved.

Google Scholar: [Author Only](#) [Title Only](#) [Author and Title](#)

McLellan H, Boevink PC, Armstrong MR, Pritchard L, Gomez S, Morales J, Whisson SC, Beynon JL, Birch PR (2013) An RxLR effector from *Phytophthora infestans* prevents re-localisation of two plant NAC transcription factors from the endoplasmic reticulum to the nucleus. PLoS Pathog. 9: e1003670.

Pubmed: [Author and Title](#)

Google Scholar: [Author Only](#) [Title Only](#) [Author and Title](#)

Melech-Bonfil S, and Sessa G (2010) Tomato MAPKKK ϵ is a positive regulator of cell-death signaling networks associated with plant immunity. Plant J. 64: 379-391.

Pubmed: [Author and Title](#)

Google Scholar: [Author Only](#) [Title Only](#) [Author and Title](#)

Moffett P, Farnham G, Peart J, Baulcombe DC (2002) Interaction between domains of a plant NBS-LRR protein in disease resistance-related cell death. EMBO J. 21: 4511-4519

Pubmed: [Author and Title](#)

Google Scholar: [Author Only](#) [Title Only](#) [Author and Title](#)

Mukhtar MS, Carvunis A-R, Dreze M, Epple P, Steinbrenner J., et al. (2011) Independently evolved virulence effectors converge onto hubs in a plant immune system network. Science 333: 596-600.

Pubmed: [Author and Title](#)

Google Scholar: [Author Only](#) [Title Only](#) [Author and Title](#)

Murphy F, He Q, Armstrong M, Giuliani LM, Boevink PC, Zhang W, Tian Z, Birch RR, Gilroy EM (2018) Potato MAP3K StVIK is required for *Phytophthora infestans* RXLR Effector Pi17316 to promote disease. Plant Physiol. 177(1): 398-410.

Pubmed: [Author and Title](#)

Google Scholar: [Author Only](#) [Title Only](#) [Author and Title](#)

Pedley KF, Martin GB (2005) Role of mitogen-activated protein kinases in plant immunity. Curr Opin Plant Biol. 8: 541-547.

Pubmed: [Author and Title](#)

Google Scholar: [Author Only](#) [Title Only](#) [Author and Title](#)

Pitzschke A, Schikora A, Hirt H (2009) MAPK cascade signalling networks in plant defence. Curr Opin Plant Biol. 12: 421-426.

Pubmed: [Author and Title](#)

Google Scholar: [Author Only](#) [Title Only](#) [Author and Title](#)

Suarez-Rodriguez MC, Adams-Phillips L, Liu Y, Wang H, Su SH, Jester PJ, Zhang S, Bent AF, Krysan PJ (2007) MEKK1 is required for fig22-induced MPK4 activation in Arabidopsis plants. Plant Physiol. 143: 661-669.

Pubmed: [Author and Title](#)

Google Scholar: [Author Only](#) [Title Only](#) [Author and Title](#)

Sun T, Nitta Y, Zhang Q, Wu D, Tian H, Lee JS, Zhang Y (2018) Antagonistic interactions between two MAP kinase cascades in plant development and immune signaling. EMBO Reports 19: e45324.

Pubmed: [Author and Title](#)

Google Scholar: [Author Only](#) [Title Only](#) [Author and Title](#)

Toruño TY, Stergiopoulos I, Coaker G (2016) Plant-pathogen effectors: cellular probes interfering with plant defenses in special and temporal manners. Ann Rev Phytopathol 54: 419-441. Wang S, Boevink PC, Welsh L, Zhang R, Whisson SC, Birch PRJ (2017) Delivery of cytoplasmic and apoplastic effectors from *Phytophthora infestans* haustoria by distinct secretion pathways. New Phytol. 216: 205-215.

Pubmed: [Author and Title](#)

Google Scholar: [Author Only](#) [Title Only](#) [Author and Title](#)

Wang S, McLellan H, Bukharova T, He Q, Murphy F, et al (2018b) *Phytophthora infestans* RXLR effectors act in concert at diverse subcellular localisations to enhance host colonization. J Exp Bot 70: 343-356.

Pubmed: [Author and Title](#)

Google Scholar: [Author Only](#) [Title Only](#) [Author and Title](#)

Wang S, Welsh L, Thorpe P, Whisson SC, Boevink PC, Birch PRJ. (2018a) The *Phytophthora infestans* haustorium is a site for secretion of diverse classes of infection associated proteins. mBio 9: e01216-18.

Pubmed: [Author and Title](#)

Google Scholar: [Author Only](#) [Title Only](#) [Author and Title](#)

Wang X, Boevink P, McLellan H, Armstrong M, Bukharova T, Qin Z, Birch PR (2015) A Host KH RNA-Binding protein is a susceptibility factor targeted by an RXLR effector to promote Late blight disease. Mol Plant 8: 1385-1395.

Pubmed: [Author and Title](#)

Google Scholar: [Author Only](#) [Title Only](#) [Author and Title](#)

Weßling R, Epple P, Altmann S, He Y, Yang L, et al. (2014) Convergent targeting of a common host protein network by pathogen effectors from three kingdoms of life. Cell Host Microbe 16: 364-375.

Pubmed: [Author and Title](#)

Google Scholar: [Author Only](#) [Title Only](#) [Author and Title](#)

Whisson SC, Boevink PC, Moleleki L, Avrova AO, Morales JG, Gilroy EM, Armstrong MR, Grouffaud S, West PV, Chapman S et al. (2007) A translocation signal for delivery of oomycete effector proteins into host plant cells. Nature 450: 115-118.

Pubmed: [Author and Title](#)

Downloaded from on June 25, 2019 - Published by www.plantphysiol.org
Copyright © 2019 American Society of Plant Biologists. All rights reserved.

Google Scholar: [Author Only](#) [Title Only](#) [Author and Title](#)

Whisson SC, Boevink PC, Wang S, Birch PR (2016) The cell biology of late blight disease. *Curr Opin Microbiol.* 34: 127-135.

Pubmed: [Author and Title](#)

Google Scholar: [Author Only](#) [Title Only](#) [Author and Title](#)

Yang L, McLellan H, Naqvi S, He Q, Boevink PC, Armstrong M, Giuliani LM, Zhang W, Tian Z, Zhan J, Gilroy EM, Birch PR (2016) Potato NPH3/RPT2-Like protein StNRL1, targeted by a *Phytophthora infestans* RXLR effector, is a susceptibility factor. *Plant Physiol.* 171: 645-657.

Pubmed: [Author and Title](#)

Google Scholar: [Author Only](#) [Title Only](#) [Author and Title](#)

Yin JL, Gu B, Huang GY, Tian Y, Quan JL, Lindqvist-Kreuze H, Shan WX (2017) Conserved RXLR effector genes of *Phytophthora infestans* expressed at the early stage of potato infection are suppressive to host defense. *Front Plant Sci.* 8: 2155.

Pubmed: [Author and Title](#)

Google Scholar: [Author Only](#) [Title Only](#) [Author and Title](#)

Zheng X, McLellan H, Fraiture M, Liu X, Boevink PC, Gilroy EM, Ying C, Kandel K, Sessa G, Birch PR, Brunner F (2014) Functionally redundant RXLR effectors from *Phytophthora infestans* act at different steps to suppress early flg22-triggered immunity. *PLoS Pathog.* 10(4): e1004057.

Pubmed: [Author and Title](#)

Google Scholar: [Author Only](#) [Title Only](#) [Author and Title](#)